

การสังเคราะห์เส้นใยนาโนพอลิอะคริลาไมด์/ไทเทเนียมที่มีแกนร่วมโดยการปั่นเส้นใย  
ด้วยไฟฟ้าสถิต

นางสาวฝากฝัน ดุริยศาสตร์

วิทยานิพนธ์นี้เป็นส่วนหนึ่งของการศึกษาตามหลักสูตรปริญญาวิทยาศาสตรมหาบัณฑิต

สาขาวิชาวิศวกรรมเคมี ภาควิชาวิศวกรรมเคมี

คณะวิศวกรรมศาสตร์ จุฬาลงกรณ์มหาวิทยาลัย

ปีการศึกษา 2555

ลิขสิทธิ์ของจุฬาลงกรณ์มหาวิทยาลัย  
บทคัดย่อและแฟ้มข้อมูลฉบับเต็มของวิทยานิพนธ์ตั้งแต่ปีการศึกษา 2554 ที่ให้บริการในคลังปัญญาจุฬาฯ (CUIR)  
เป็นแฟ้มข้อมูลของนิสิตเจ้าของวิทยานิพนธ์ที่ส่งผ่านทางบัณฑิตวิทยาลัย

The abstract and full text of theses from the academic year 2011 in Chulalongkorn University Intellectual Repository (CUIR)  
are the thesis authors' files submitted through the Graduate School.

SYNTHESIS OF POLYACRYLONITRILE/TITANIA CO-AXIAL  
NANOFIBERS VIA ELECTROSPINNING

Miss Farkfun Duriyasart

A Thesis Submitted in Partial Fulfillment of the Requirements  
for the Degree of Master of Engineering Program in Chemical Engineering  
Department of Chemical Engineering  
Faculty of Engineering  
Chulalongkorn University  
Academic Year 2012  
Copyright of Chulalongkorn University

Thesis Title                   SYNTHESIS OF POLYACRYLONITRILE/TITANIA CO-  
  AXIAL NANOFIBERS VIA ELECTROSPINNING  
By                                 Miss Farkfun Duriyasart  
Field of study                 Chemical Engineering  
Thesis Advisor               Assistant Professor Varong Pavarajarn, Ph.D.

---

Accepted by Faculty of Engineering, Chulalongkorn University in Partial  
Fulfillment of the Requirements for the Master's Degree

..... Dean of the Faculty of Engineering  
(Associate Professor Boonsom Lerdhirunwong, Dr.Ing.)

THESIS COMMITTEE

..... Chairman  
(Assistant Professor Anongnat Somwangthanaroj, Ph.D.)

..... Thesis Advisor  
(Assistant Professor Varong Pavarajarn, Ph.D.)

..... Examiner  
(Associate Professor Tawatchai Charinpanitkul, D.Eng.)

..... Examiner  
(Assistant Professor Apinan Soottitantawat, D.Eng.)

..... External Examiner  
(Chanchana Thanachayanont, Ph.D.)

ฝากฝัน ดุษฎีสารคดี : การสังเคราะห์เส้นใยนาโนพอลิอะคริโลไนไตรล์/ไทเทเนียที่มีแกนร่วมโดย  
 การปั่นเส้นใยด้วยไฟฟ้าสถิต (SYNTHESIS OF POLYACRYLONITRILE/TITANIA CO-  
 AXIAL NANOFIBERS VIA ELECTROSPINNING) อ.ที่ปรึกษาวิทยานิพนธ์หลัก :  
 ผศ.ดร.วรงค์ ปวรอาจารย์, 73 หน้า

เส้นใยนาโนของไทเทเนียที่มีแกนพอลิเมอร์สามารถสังเคราะห์ได้สำเร็จจากเทคนิคร่วมของกระบวนการ  
 โซล-เจลและการปั่นเส้นใยด้วยไฟฟ้าสถิตแบบแกนร่วมโดยใช้พอลิอะคริโลไนไตรล์ในไดเมทิลฟอร์ไมด์เป็นสาร  
 ละลายแกนและไทเทเนียโซลซึ่งเตรียมได้จากไทเทเนียมเตตระไฮดรอกไซด์, ไดเมทิลฟอร์ไมด์, กรดอะซิติก  
 และพอลิไวนิลไพโรลิโดนเป็นสารละลายส่วนเปลือก สำหรับเทคนิคการปั่นเส้นใยด้วยไฟฟ้าสถิตแบบแกนร่วมใน  
 งานวิจัยนี้ สารละลายส่วนแกนและสารละลายส่วนเปลือกจะถูกป้อนแยกกันเข้าสู่หัวฉีดแบบแกนร่วม งานวิจัยนี้  
 ได้ศึกษาอิทธิพลของอัตราการไหลของทั้งสารละลายส่วนแกนกับสารละลายส่วนเปลือกและศักย์ไฟฟ้าที่ให้ เส้น  
 ผ่านศูนย์กลางของเส้นใยที่ปั่นได้มีค่ามากขึ้นเมื่ออัตราการไหลของสารละลายแกนสูงขึ้น เส้นใยที่มีขนาดเส้นผ่าน  
 ศูนย์กลางสม่ำเสมอเฉลี่ย 380 นาโนเมตร สามารถผลิตได้จากการให้ศักย์ไฟฟ้า 22 กิโลโวลต์ในกระบวนการปั่น  
 เส้นใยด้วยไฟฟ้าสถิตในขณะที่อัตราการไหลของสารละลายส่วนแกนและส่วนเปลือกเป็น 1.2 มิลลิลิตรต่อชั่วโมง  
 และ 0.9 มิลลิลิตรต่อชั่วโมงตามลำดับ โครงสร้างแกน-เปลือกของเส้นใยที่ปั่นได้ได้รับการยืนยันโดยใช้กล้อง  
 จุลทรรศน์อิเล็กตรอนแบบส่องผ่าน จากนั้นเส้นใยแกนร่วมที่ปั่นได้จึงถูกเผาในอากาศโดยพบว่าการเกิดผลึกของ  
 ไทเทเนียและการกำจัดพอลิไวนิลไพโรลิโดนนั้นขึ้นอยู่กับอุณหภูมิที่ใช้ในการเผาเส้นใย แกนพอลิอะคริโลไนไตรล์  
 ซึ่งสามารถทนต่ออุณหภูมิได้สูงกว่าพอลิไวนิลไพโรลิโดนทำให้เส้นใยไทเทเนียที่ได้มีความยืดหยุ่น นอกจากนี้ยัง  
 พบว่าสามารถผลิตเส้นใยนาโนของไทเทเนียที่มีสองเฟสได้จากการเผาที่อุณหภูมิ 450 องศาเซลเซียส

ภาควิชา..... วิศวกรรมเคมี .....ลายมือชื่อนิสิต.....

สาขาวิชา..... วิศวกรรมเคมี .....ลายมือชื่อ อ.ที่ปรึกษาวิทยานิพนธ์หลัก.....

ปีการศึกษา.....2555.....

## 5370463021: MAJOR CHEMICAL ENGINEERING

KEYWORDS: TITANIA/NANOFIBER/ELECTROSPINNING/CO-AXIAL

FARKFUN DURIYASART: SYNTHESIS OF POLYACRYLONITRILE/TITANIA  
CO-AXIAL NANOFIBERS VIA ELECTROSPINNING ADVISOR:  
ASST.PROF.VARONG PAVARAJARN, Ph.D., 73 pp.

Titania nanofibers having polymer core were successfully prepared via the combination of sol-gel and co-axial electrospinning techniques, using polyacrylonitrile (PAN) in dimethyl formamide (DMF) as core solution and titania sol derived from titanium(IV) isopropoxide (TTIP), DMF, acetic acid and poly vinyl pyrrolidone (PVP) as sheath solution. For the co-axial electrospinning technique in this research, the core solution and the sheath solution were supplied separately to a co-axial nozzle. The effects of the flow rate of both core solution and sheath solution, and the electric potential applied were investigated in this research. The diameter of the electrospun fiber is increased when the flow rate of the core solution is increased. The uniform fibers with an average diameter of 380 nm could be fabricated by applying the electric potential of 22 kV on the co-axial electrospinning system, while the flow rate of the core solution and the sheath solution were 1.2ml/h and 0.9 ml/h, respectively. The core-sheath structure of the electrospun fibers was confirmed by using transmission electron microscopy. The electrospun co-axial fibers were then subjected to the calcination process. The crystallization of titania and the removal of PVP were found to depend upon the calcination temperature of the electrospun fibers. The presence of PAN core, which can withstand higher temperature than PVP, can provide flexibility to the final titania nanofibers. It is found that the biphasic titania nanofibers products with an average diameter of 150 nm can be obtained after calcination at 450 °C.

Department: ...Chemical Engineering.....Student's Signature.....

Field of Study: Chemical Engineering.....Advisor's Signature.....

Academic Year: .2012.....

## ACKNOWLEDGEMENTS

This thesis could not have been complete without my academic advisor. Assistant Professor Dr. Varong Pavarajarn, who encouraged and gave useful suggestions and discussion through my academic program. Thank you. I would also be grateful to Assistant Professor Dr. Anongnat Somwangthanoj, as the chairman, Associate Professor Dr. Tawatchai Charinpanitkul, Dr. Apinan Suttitantawat and Dr. Chanchana Thanachayanont, as the members of thesis committee.

In addition, I would like to thank Professor Fuji Masayashi for give me an opportunity for doing research abroad, and his laboratory members for everything in Japan.

Most of all, I would like to express my deepest gratitude to my family who always pay attention to me all the times, I could not have a chance to do what I am doing without them. The most success of graduation is devoted to my family.

Last but not least, I wish to thank all the members of the Center of Excellence in Particle technology, Department of Chemical Engineering, Faculty of Engineering, Chulalongkorn University for their assistance.

## CONTENTS

		<b>Page</b>
ABSTRACT (THAI).....		iv
ABSTRACT (ENGLISH).....		v
ACKNOWLEDGEMENTS.....		vi
CONTENTS.....		vii
LIST OF TABLES.....		x
LIST OF FIGURES.....		xi
CHAPTER I	INTRODUCTION.....	1
CHAPTER II	THEORY AND LITERATURE REVIEWS.....	3
	2.1 Physical Properties of Materials Used.....	3
	2.1.1 Titania.....	3
	2.1.2 Polymers.....	5
	2.2 Fabrication of Titania/Polyacrylonitrile Co-axial Fibers.....	6
	2.2.1 Sol-gel process.....	6
	2.2.2 Electrospinning.....	9
	2.2.3 Co-axial Electrospinning.....	11
	2.2.3.1 Principle of co-axial electrospinning.....	11
	2.2.3.2 Parameters in electrospinning technique.....	13
CHAPTER III	EXPERIMENT.....	20
	3.1 Chemicals.....	20
	3.2 Electrospinning Apparatus.....	20
	3.3 Experimental Procedures.....	21
	3.3.1 Preparation of electrospinning solutions.....	21
	3.3.2 Co-axial electrospinning process.....	22
	3.3.3 Calcination of the PAN-TiO <sub>2</sub> /PVP core-sheath fibers.....	22
	3.4 Characterization of Products.....	22
	3.4.1 Scanning electron microscopy (SEM).....	22

	<b>Page</b>
3.4.2	Transmission electron microscopy (TEM).....23
3.4.3	Rheometer.....23
3.4.4	Thermogravimetric analysis (TGA).....23
3.4.5	Fourier-transform infrared spectroscopy (FT-IR).....23
3.4.6	X-ray diffraction analysis (XRD).....24
3.4.7	Universal testing machine (UTM).....24
CHAPTER IV	RESULTS AND DISCUSSION.....25
4.1	Core-Sheath Structure Formation of PAN/PVP Fibers.....25
4.2	Co-axial Electrospinning of PAN/TiO <sub>2</sub> (PVP) Fibers.....29
4.2.1	Effects of solution flow rate.....31
4.2.2	Effects of electric potential.....33
4.3	Core-Sheath Structure of PAN/Titania Fibers.....37
4.3.1	Thermal Gravimetric Analysis (TGA).....37
4.3.2	Effect of calcination process on the co-axial fibers.....40
4.3.3	Observation of fiber cross section by TEM.....44
4.3.4	Fourier transform infrared spectroscopy (FT-IR) analysis.....46
4.3.5	Energy-dispersive X-ray spectroscopy (EDX).....50
4.4	Crystal Structure of Titania in Core-Sheath Fibers.....52
4.5	Flexibility of PAN/TiO <sub>2</sub> Core-Sheath fibers.....54
CHAPTER V	CONCLUSIONS AND RECOMMENDATIONS.....57
5.1	Summary of The Results.....57
5.2	Conclusions .....57
5.3	Recommendations for the Future Studies .....58
REFERENCES	.....59



APPENDICES.....	65
APPENDIX A    TGA THERMOGRAMS OF PAN AND PVP.....	66
APPENDIX B    EFFECT OF TIME ON THE VISCOSITY OF SHEATH SOLUTION.....	68
APPENDIX C    EFFECT OF AGING OF SHEATH SOLUTION ON THE MORPHOLOGY OF FIBERS.....	69
APPENDIX D    EFFECT OF WORKING DISTANCE ON THE CO-AXIAL FIBER MORPHOLOGY.....	70
APPENDIX E    EFFECT OF ROTATING DRUM COLLECTOR ON FIBERS MORPHOLOGY.....	71
APPENDIX F    LIST OF PUBLICATION.....	72
VITA .....	73

## LIST OF TABLES

	<b>Page</b>
Table 2.1 Crystallographic properties of anatase, brookite and rutile.....	4
Table 4.1 Ratio of the core diameter to the fiber diameter of different concentration of PAN and PVP solutions.....	29

## LIST OF FIGURES

<b>Figure</b>	<b>Page</b>
2.1 Crystal structures of TiO <sub>2</sub> ; Anatase (a), Rutile (b) and Brookite (c).....	4
2.2 Reaction pathway of titania sol in PVP solution.....	6
2.3 Simplified chart of sol-gel process.....	7
2.4 Schematic of co-axial electrospinning set up and the compound taylor cone.....	12
2.5 Schematic of the voltage dependence of the core-sheath fiber formation.....	12
2.6 TEM image of electrospun silk/ poly(ethylene oxide) core-sheath fiber.....	13
2.7 Effect of core solution concentration on the fiber diameter.....	14
2.8 TEM images of miscible core solution and sheath solution.....	15
2.9 TEM images of Li and Xia research hollow fiber from mineral oil core solutio and Ti(OiPr <sub>4</sub> )/PVP sheath solution, and porous fiber from miscible PS/DMF/THF core solution in Ti(OiPr <sub>4</sub> )/PVP sheath solution.....	16
2.10 TEM images of Li and Xia 's hollow fiber of Ti(OiPr <sub>4</sub> )/PVP under higher voltage and lower voltage, split jets from PCL core and gelatin sheath solution when the voltage is too high.....	17
2.11 Compound cone formed when the sheath flow rate is constant and while the core flow is increased.....	18
3.1 Schematic of an electrospinning setup.....	21
4.1 SEM images of products of PAN solution and PVP solution whereas the concentrations of PVP and PAN solutions are 10/6, 10/8, and 10/10 %wt/%wt.....	26
4.2 Viscosity of PVP and PAN polymer solution at different concentration.....	26
4.3 TEM micrographs of products obtained from co-axial electrospinning of PAN solution and PVP solution using applied potential of 22 kV and the distance from nozzle to collector of 22 cm, whereas the concentrations of PAN and PVP solutions are 8/10, 8/13 and 8/15 wt%/wt%.....	27
4.4 Viscosity curve of titania precursor solution prepared from PVP solution concentration of 24wt%, 18wt%, 14wt% and 12wt%	

<b>Figure</b>	<b>Page</b>
compared with 10wt% PVP solution used as sheath solution in PAN/PVP co-axial electrospinning.....	30
4.5 TEM of PAN/titania(PVP) co-axial electrospun fiber.....	31
4.6 SEM images of products obtained from co-axial electrospinning of PAN solution and PVP/titania solution using applied potential of 22 kV and the distance from nozzle to collector of 22 cm, whereas the flow rate of PAN and PVP/titania solutions are 1.2/0.9 (a), 1.2/1.2 (b), 1.2/1.5 (c), 0.9/1.2 (d), 1.2/1.2 (e), 1.5/1.2 (f) (ml/h)/(ml/h).....	32
4.7 Taylor cone at the tip of co-axial nozzle when electric potential applied.....	33
4.8 SEM images of the products obtained from the co-axial electrospinning of PAN solution and PVP/titania solution with the tip-to-collector distance of 22 cm and the applied electric voltage are 20 kV, 21 kV and 22 kV.....	34
4.9 Histogram of diameter size distributions of PAN/TiO <sub>2</sub> (PVP) co-axial fibers obtained from the co-axial electrospinning of PAN solution and PVP/titania solution with the tip-to-collector distance of 22 cm and the applied electric voltage 20 kV, 21 kV and 22 kV.....	35
4.10 Diameter size with deviation of PAN/TiO <sub>2</sub> (PVP) co-axial fibers obtained from the co-axial electrospinning of PAN solution and PVP/titania solution with the tip-to-collector distance of 22 cm and the applied electric voltage 20 kV, 21 kV and 22 kV.....	36
4.11 TGA curve of PAN/PVP(titania) co-axial electrospun fibers.....	37
4.12 TGA curve of PAN and PVP electrospun fibers.....	38
4.13 DSC curve of PAN/PVP(titania) co-axial electrospun fibers.....	39
4.14 SEM images of the products obtained from the co-axial electrospinning of PAN solution and PVP/titania solution with the tip-to-collector distance of 22 cm and the applied electric voltage of 22 kV, before and after calcination at 450 °C for 2 h.....	40
4.15 Histogram of diameter size distribution of as-spun PAN/TiO <sub>2</sub> (PVP) co-axial fibers and PAN/TiO <sub>2</sub> co-axial fibers after calcination at 450 °C for 2 h.....	41

<b>Figure</b>	<b>Page</b>
4.16 SEM images of the fibers obtained from the calcination of co-axial electrospun fiber of PAN solution and PVP/titania solution with the tip-to-collector distance of 22 cm and the applied electric voltage of 22 kV, before and after calcination at 300 °C, 450 °C and 800 °C.....	42
4.17 SEM images of 800 °C calcined fibers from PAN/TiO <sub>2</sub> (PVP) co-axial fibers and from TiO <sub>2</sub> (PVP) simple fibers .....	43
4.18 Diameter size with deviation of PAN/TiO <sub>2</sub> (PVP) co-axial fibers at different calcination temperature.....	43
4.19 TEM image of cross-section of PAN/titania co-axil fiber and PAN/titania coaxial fibers.....	44
4.20 The possible cross sectional image of co-axial fibers.....	45
4.21 TEM image of cross-section of PAN/titania(PVP) as-spun co-axial fiber.....	45
4.22 FT-IR spectrum of PAN as-spun fiber and PAN/TiO <sub>2</sub> co-axial fiber.....	47
4.23 The possible degradative path and cyclization of PAN heated at various temperature proposed by Peikai Miao et al.....	47
4.24 FT-IR spectrum of PAN as-spun fiber and PAN fiber after calcination at 200°C, 350°C and 400°C.....	48
4.25 EDX map of TiO <sub>2</sub> fibers after the calcination of PAN/TiO <sub>2</sub> (PVP) at 800 °C.....	50
4.26 EDX analysis of PAN titania co-axial fibers after the calcination at 450 °C.....	51
4.27 XRD patterns of the PAN/titania(PVP) core-sheath fibers calcined for 2 h at 450°C and 500 °C.....	52
4.28 XRD patterns of the calcined PVP/titania fiber at 450 °C for 2h using EtOH and DMF as a solvent in the spinning solution.....	53
4.29 Stress-strain curves of PAN/TiO <sub>2</sub> (PVP) as-spun co-axial fibers and PAN/TiO <sub>2</sub> co-axial fibers.....	54
4.30 PAN/titania co-axial fibers and titania fiber after calcinations at temperature of 450 °C.....	55
A.1 TGA thermogram of PAN fiber.....	66
A.2 TGA thermogram of PAN powder.....	66

<b>Figure</b>	<b>Page</b>
A.3 TGA thermogram of PVP fiber.....	67
A.4 TGA thermogram of PVP powder.....	67
B.1 Viscosity curve of titania(PVP) sheath solution.....	68
C.1 SEM images of the products obtained from the co-axial electrospinning of PAN solution and PVP/titania solution using as prepared (a) and after aged for a day (b) before electrospinning process.....	69
D.1 SEM images of the products obtained from the co-axial electrospinning of PAN solution and PVP/titania solution with and the applied voltage of 22 kV and the tip-to-collector distance are 16 cm,19 cm and 22 cm.....	70
E.1 SEM image of PAN/titania co-axial fibers using rotating drum collector.....	71

# CHAPTER I

## INTRODUCTION

Water pollution from organic chemicals, which are used in agriculture, is one of the important problems of agricultural countries since pesticide and fertilizer are increasingly used in farming process for preventing insect infestation and for improving the products quality, respectively. However, using those chemicals leads to the contamination of water resource. Some of the contaminants are toxic, which could be harmful to human and animals. Thus, the removal of the toxicant is needed. There are many kinds of water treatments, one of that is a photocatalytic degradation of organic compound using titanium (IV) oxide as a catalyst. This photodegradation is a natural process, which has been observed and harnessed to work in an induced environment.

Titanium (IV) oxide or titania particle is a common material used in many industries due to its various properties, such as transparency to visible light, high refractive index, low absorption coefficient and capability of photocatalytic degradation of organic materials. Titania electrode was found to be a catalyst in the photodegradation of organic compounds since 1972 by Fujishima et al [1]. After that, many researchers have reported the studies of photocatalytic behavior of titania. The catalytic activity of titania increases as the size of titania particles approaches nanometered scale due to the increasing of the surface area [2-4]. However, nanoparticles are difficult to be handled and difficult to be removed from water after the reaction is complete, therefore titania nanofibers consisting of nanosized grains are preferred.

Titania nanofiber can be synthesized by several methods including sol-gel, dip-coating and electrochemical methods. One of the techniques that have been used to produce nanofibers is electrospinning technique. In many research works, the sol-gel method combining with an electrospinning technique has been used to fabricate titania nanofibers [5-8]. Nevertheless, although titania nanofibers can be handled easier than titania in nanoparticles form, titania nanofibers are brittle and can be

crumbled into powder after repeated uses. For solving this problem, coaxial nanofibers which is made of polymer core, covering by titania will make the fibers become flexible.

Electrospinning is a notable technique often use for nanofiber fabrication according to it simply preparation. In typical electrospinning process, a charged solution or melt flowing out of capillary is drawn by stretch, using a strong electric field, to obtain nanofibers in the form of nonwoven mesh. Under optimum solution or melt material properties and spinning condition, fiber of the order of 100 nm could be obtained [9].

Co-axial electrospinning is one of many techniques modified from electrospinning technique in recent years in order to enhance the quality and improve the functionality of the resulting nanofiber structure. In the co-axial electrospinning process, two different materials are delivered independently through a co-axial capillary and drawn to generate nanofiber in core-sheath configuration [9].

In this research, the sol-gel method is combined with co-axial electrospinning technique forming titania nanofiber with polymer core. Polyacrylonitrile is considered to be a core material of the fiber because of its high decomposition temperature compared with polyvinyl pyrrolidone which is used in sol-gel process of titania [6, 10-12].

The main focus of this work is how to synthesize the uniform titania nanofiber having polyacrylonitrile core by adjusting parameters in sol-gel and electrospinning process that affect the resulting fibers.

This thesis is divided into five chapters. The first two chapters describe general information as an introduction and objective of the research in Chapter I, while theory related to this work and literature reviews are explained in Chapter II. Chapter III presents materials and the experimental procedure. Chapter IV shows the results and discussion. Chapter V is the last chapter, which concludes the results and gives some recommendation for future works.



## CHAPTER II

### THEORY AND LITERATURE REVIEWS

This chapter will explain about the theory relating to properties of materials, which are used in this research such as titanium (IV) oxide (titania), polyacrylonitrile (PAN), polyvinyl pyrrolidone (PVP). The theory relating to the synthesis method will also be described.

#### 2.1 Physical Properties of Materials Used

##### 2.1.1 Titania

Titanium (IV) oxide or titania is a material having great potential for various industrial applications. Therefore, the fabrication of titania has been focused in numerous researches. Titania has been used as catalyst, catalyst support, electronic components, cosmetic pigment and filter coating [13-17]. In recent years, the main attention of titania fabrication has been devoted to its photocatalytic activity. Titania has relatively wide band gap (3.2 eV for anatase), which means that UV light can excite anatase titania to generate charge carriers, i.e. electron and holes. Accordingly, highly reactive radicals are generated and oxidation-reduction of species adsorbed on the surface of titania can occur [18].

Naturally, titania occurs in three crystalline forms; i.e. anatase form which tends to be more stable at low temperature and can be transformed into rutile form under high temperature, brookite which is rare and usually found only in minerals, and rutile which is most common natural form. Rutile titania is thermally stable form, which is frequently found in igneous rocks. All three forms of titania have been prepared artificially. However, only rutile has been obtained in the form of transparent large single crystal. The structure of each titania crystalline form is shown in Figure 2.1 and a summary of the crystallographic properties of all forms are given in Table 2.1.

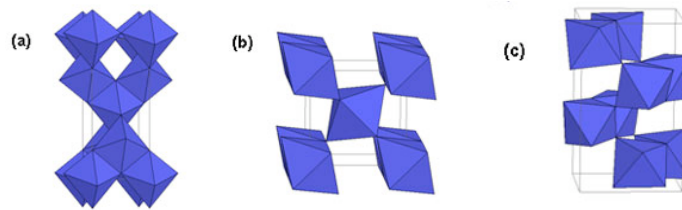


Figure 2.1 Crystal structures of TiO<sub>2</sub>; Anatase (a), Rutile (b) and Brookite (c)

Table 2.1 Crystallographic properties of anatase, brookite and rutile [19]

	<i>Anatase</i>	<i>Brookite</i>	<i>Rutile</i>
Crystal structure	Tetragonal	Orthorombic	Tetragonal
Density, [g/cm <sup>3</sup> ]	3.9	4.23	4.23
Hardness, [Mohs scale]	5 <sup>1/2</sup> - 6	5 <sup>1/2</sup> - 6	7 - 7 <sup>1/2</sup>
Unit cell	D <sub>4h</sub> <sup>19</sup> .4TiO <sub>2</sub>	D <sub>2h</sub> <sup>15</sup> .8TiO <sub>2</sub>	D <sub>4h</sub> <sup>12</sup> .3TiO <sub>2</sub>
Lattice parameters, [nm]			
<i>a</i>	0.3758	0.9166	0.4584
<i>b</i>		0.5436	
<i>c</i>	0.9514	0.5135	2.953

The important commercial forms of titania are anatase and rutile which are tetragonal. Anatase usually occurs in near-regular octahedral. Rutile forms slender prismatic crystal, which are frequently twinned. Thus, both anatase and rutile are anisotropic and their physical properties, e.g. refractive index, change according to the direction relative to the crystal axes. However, the distinction between

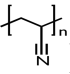
crystallographic directions is lost in most applications due to the random orientation of large numbers of small particles.

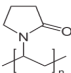
Rutile phase of titania is thermodynamically stable at room temperature, while anatase is metastable. Transformation of phase from anatase to rutile can occur with very slow rate at room temperature. Macroscopic change of phase can occur at appreciable rate at temperature higher than 800 °C. On the other hand, Nanosized grains of anatase titania can be appreciably changed to rutile phase at temperature higher than 400 °C [20-22].

Titania is thermally stable with melting point of 1855°C and has high resistance to chemical attack. When it is heated under vacuum, there is a chance of slight loss in oxygen atom that results in a change in composition to TiO<sub>1.97</sub>. The product is dark blue but can be reverted to the original white color when it is heated in air [23].

### 2.1.2 Polymers

Two polymers were used for core part and sheath part of co-axial fiber. Polyacrylonitrile was used as a core material to increase the flexibility of the co-axial fibers. Another polymer is polyvinyl pyrrolidone that was used in the preparation of titania precursor sol for producing the sheath part of the fiber.

Poly acrylonitrile () or PAN is a synthetic polymer having high degradation temperature compared with other polymers. Since PAN is most commonly used in fiber form, many researches reported the fabrication of PAN fibers by electrospinning technique. E.g. Wang *et al.* (2006) reported the effects of polymer concentration and electrospinning parameters on nano fiber of PAN [24].

Poly vinyl pyrrolidone () or PVP is a thermoplastic. High molecular weight PVP have been used as a polymer media in titania sol preparation to increase the viscosity of the solution for electrospinning process in many works. PVP can be dissolved in polar solvents such as water and ethanol, which are frequently used in the

preparation of titania sol. Moreover, PVP helps the dispersion of titania precursor in titania sol by forming complexation at an active group of PVP [25]. The reaction pathway of titania sol from titanium tetraisopropoxide, acetic acid and PVP was proposed as shown in Figure 2.2.

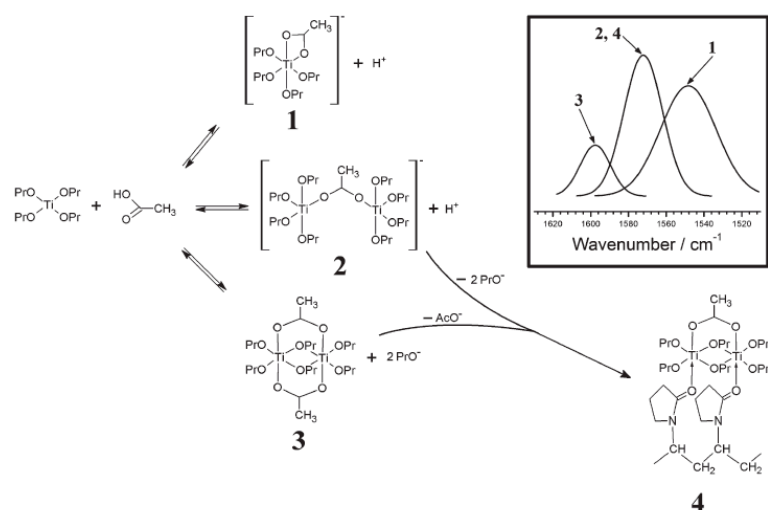


Figure 2.2 Reaction pathway of titania sol in PVP solution proposed by Skotak *et al* [25].

Another reason why poly PVP is commonly used in the preparation of titania sol for electrospinning process is that the removal of PVP from the fiber can be done at lower temperature than crystallization of amorphous titania to anatase. Therefore, poly vinyl pyrrolidone in sheath structure of the co-axial as-spun fiber could be decomposed prior to the crystallization temperature.

## 2.2 Fabrication of Titania/Polyacrylonitrile Co-axial Fibers

### 2.2.1 Sol-gel process

Sol-gel reaction is a common technique used in the synthesis of metal (semi-metal) oxide compounds [26]. Sol-gel process involves the formation of sol followed by that of gel. The process starts from a chemical solution or sol that acts as precursor for an integrated network or gel of either discrete particles or network polymers. Sol; a suspension solid in liquid with particle size ranging from 1 nm to 1  $\mu$ m, can be

obtained by hydrolysis and partial condensation of a precursor such as inorganic salt or metal alkoxide. Further condensation of sol particles into a three-dimensional network produces gel, which is a diphasic material with a solid encapsulating liquid or solvent. Alternatively, destabilizing the solution of preformed sols can also produce gel. These materials are referred to be aquasol or aquagel if water is used as solvent, and alcosol or alcogel if alcohol is used.

By applying the sol-gel process, it is possible to fabricate advanced materials in a wide variety of forms, e.g. ultra-fine or spherical shaped powders, thin film coatings, fibers, microporous membranes, monolithic materials and porous aerogel materials as shown in Figure 2.3.

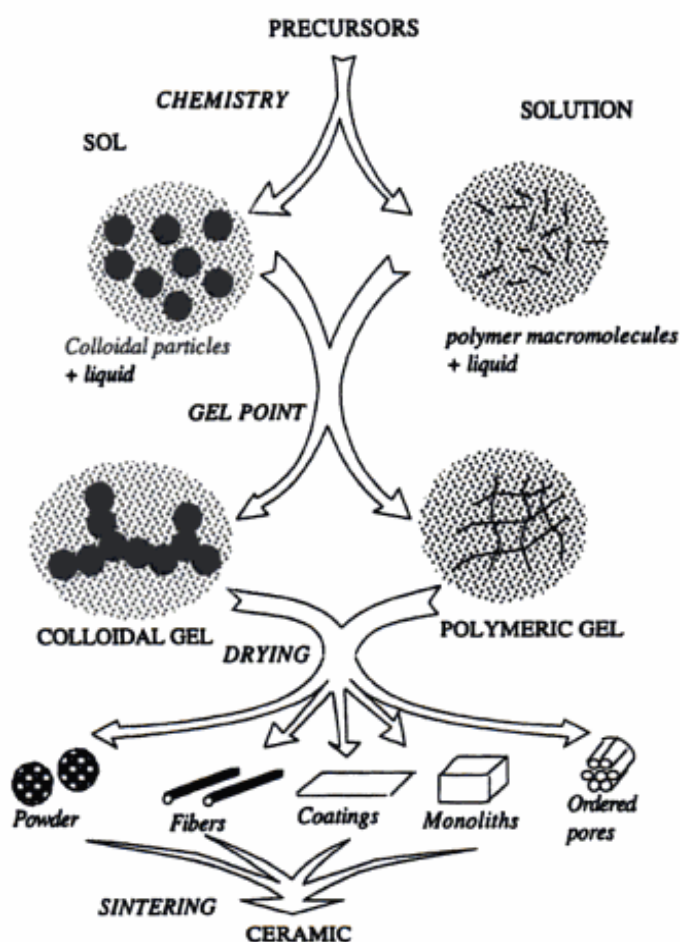
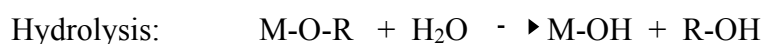


Figure 2.3 Simplified chart of sol-gel process.

The precursor in sol-gel preparation can either be metal salt/alkoxide dissolved in appropriate solvent or stable colloidal suspension of preformed sols. Metal alkoxides have been most extensively used because they are commercially available in high purity and their solution chemistry has been well documented. At its simplest level, sol-gel chemistry with metal alkoxide can be described in terms of two classes of reaction:



where M and R are metal atom and alkyl group, respectively.

Because hydrolysis and condensation are both nucleophilic displacement reactions, the reactivity of metal alkoxides depends on the positive charge of partially charged metal atom and its coordination number. For example, tetraethyl orthosilicate (TEOS) is the least reactive comparing with common alkoxides because of the small positive partial charge on silicon. Thus, the longer and bulkier the alkoxide group attaching to a particular metal atom, the less reactive in hydrolysis and condensation of that precursor is. Therefore, changing type of precursor and/or its concentration are effective means toward controlling the reaction rates.

For sol-gel parameters, an important parameter affecting the reaction rate is temperature, which can be adjusted to increase or decrease rate of reaction. Type of solvent can affect the condensation reaction directly. It is also possible to prepare gel without solvent as long as another mean, such as ultrasound irradiation, is used to homogenize an otherwise immiscible alkoxide/water mixture. Another parameter called gelation time, which is defined as the time that the solution undergoes rapid rising in viscosity, is corresponding to the transition from viscous fluid to elastic gel. At the gel point, the solid phase forms a continuous structure that reflects the formation and branching of particles under specific growth condition. This particular

phase is important because it is the genesis of structural evolution that takes place in all subsequent processing steps [27].

Generally, titania synthesis via the sol-gel technique starts with mixing titania alkoxide with alcohol. Then, acid solution is added to the mixture [28]. It was found that PAN polymer used in this research precipitated in alcohol, thus DMF would be used as a solvent.

### **2.2.2 Electrospinning**

Before considering the co-axial electrospinning technique, we should know about the conventional electrospinning first. Electrospinning has been recognized as a simple technique, which involves polymer science, electrical engineering, mechanical engineering, material engineering and rheology. Electrospinning technique produces fibers with diameter in the range of nanometer to micrometer. The conventional process consists of applying electrical potential between a grounded collector and a droplet of polymer solutions or melt held at the end of capillary tube because of its surface tension. As the voltage is increased, charge is induced on the surface of fluid. When the applied electric field overcomes the surface tension of the droplet, the droplet is distorted forming a conical shape, commonly referred to as the Taylor cone. Then, a charged jet of the solution or melt is ejected from the apex of a conical shape, then the jet grows longer and thinner due to bending instability or splitting [29, 30]. While the jet travels toward to a collector, the solvent evaporates or the polymer solidifies and randomly deposited as a non-woven on the collector [31].

Important features of electrospinning are:

- (a) Suitable solvent should be available for dissolving the polymer.
- (b) The vapor pressure of the solvent should be suitable; the solvent should evaporate quickly enough for maintaining the fiber integrity when it reaches the target but not too quickly to allow the fiber reaching the nanometer range.

- (c) The viscosity and surface tension of the solvent must neither be too large nor too small to allow the polymer solution to form Taylor cone at the tip of the nozzle.
- (d) The power supply should be adequate to overcome the viscosity and surface tension of the polymer solution to form and to sustain the jet from the tip.
- (e) The gap between the tip of the nozzle containing fluid and grounded surface should not be too small to prevent a spark between the electrodes, yet it should be large enough for the evaporation of solvent during the fibers formation.

The electrospinning process produces fibers with diameter in the range of one or two order of magnitude smaller than that of conventional textile fibers. The small diameter provides large surface area-to-mass ratio, in the range of  $10 \text{ m}^2/\text{g}$  (fiber diameter is around 500 nm) to  $1000 \text{ m}^2/\text{g}$  (fiber diameter is around 50 nm). The equipment required for electrospinning is simple and only a small amount of polymer sample is needed to produce nanofibers.

In this research, synthesis of titania nanofibers with polymer core is considered. Titania nanofibers synthesized by electrospinning process has been studied in several researches. As previously mentioned, PVP is usually considered to be the spinning aid for titania electrospinning. Li *et al.* (2003) studied fabrication of titania nanofibers by electrospinning with controllable diameter and porous structures. When the solution containing both PVP ( $M_w \sim 1,300,000$ ) and titanium tetraisopropoxide in ethanol was injected through a needle under strong electric field, composite nanofibers made from PVP and amorphous titania were formed as a result of electrostatic jetting. These nanofibers could be then converted into fibers of anatase titania without changing their morphology via calcination in air at  $500^\circ\text{C}$ . The average diameter of these fibers could be controlled in a range from 20 to 200 nm. It was found that, after calcined, the fibers remained as continuous structures with their average diameter reduced due to the loss of PVP from the nanofibers and the crystallization of titania. Moreover, they reported effects of parameters in the process, i.e. the diameter of the nanofibers was increased as the PVP concentration was



increased, thinner nanofibers were obtained when the strength of electric field was increased, faster feeding rate of PVP solution often resulted in increasing of fibers diameter and the low concentration of PVP solution led to the formation of thinner ceramic nanofibers [32]. Afterward, Tekman *et al.* (2008) prepared titania nanofibers with uniform diameter in a range of 54-78 nm by electrospinning technique applied from that of Li *et al.*, using PVP ( $M_w \sim 1,300,000$ ), titanium isopropoxide and acetic acid in ethanol for electrospinning solution, then calcined at 600°C. They also reported that viscosity of the prepared sol did not affect the fibers morphology but the increasing electric field caused bead formation and discontinuity in nanofiber morphology [6].

Even though titania nanofibers could be used as photocatalyst in photodegradation [12], titania nanofibers are brittle and can be crumble into powder after repeated uses. Thus, titania fiber with polymer core or polymer fabricated from co-axial electrospinning technique is considered in this work.

### **2.2.3 Co-axial Electrospinning**

Co-axial electrospinning technique is used by combining with sol-gel process to produce co-axial fibers of  $\text{TiO}_2/\text{PAN}$  in this work. Theory relating to this process is presented as followed.

#### *2.2.3.1 Principle of co-axial electrospinning*

Co-axial electrospinning is one of many techniques modified from electrospinning technique in recent years in order to enhance the quality and improving the functionality of the resulting nanofiber structure. The principle of co-axial electrospinning is similar to that of the conventional electrospinning. In the co-axial electrospinning process, two different materials are used in producing core part and sheath part of the fiber. The core material and sheath material are delivered independently through a co-axial capillary forming compound droplet, which is shown in Figure 2.4. The compound droplet is charged after the high voltage is supplied. Charges are induced on the surface of sheath fluid predominantly as suggested by Greiner *et al.* (2006) [33]. Above the critical value of electrical potential

supplied, fluid droplet will be distorted via repulsive force of charges, resulted in small jet forming from the compound cone of materials. Li and Xia (2004) explained that rapid stretching of the sheath material can create strong viscous stress inside sheath fluid and will be transferred to the core material. The core part will be stretched and elongated by the shear stress at the interface between core part and sheath part as shown in Figure 2.5 [34]. These result in the formation of nanofiber in core-sheath configuration [35].

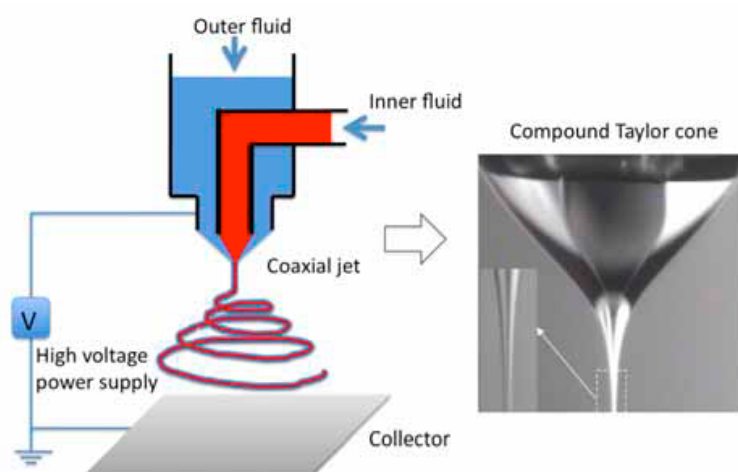


Figure 2.4 Schematic of co-axial electrospinning set up and the compound Taylor cone from Fengyu *et al.* [36] and Loscertales *et al.* [37], respectively.

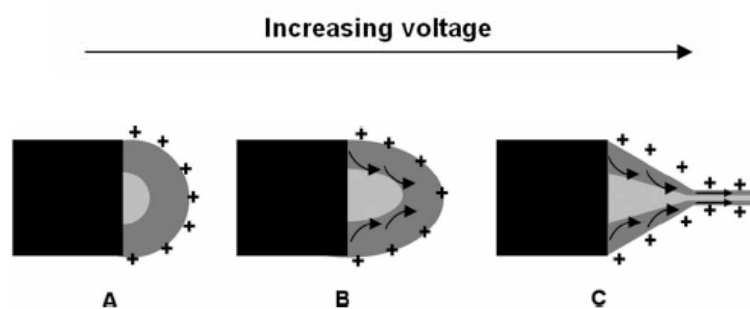


Figure 2.5 Schematic of the voltage dependence of the core-sheath fiber formation

### 2.2.3.2 Parameters in electrospinning technique

The parameters affecting the co-axial electrospinning process are classified into two kinds, material parameters and process parameters.

#### *i) Material parameters*

Properties of materials are important factors that affect the quality of the process and morphology of the fiber product. Some of them will be explained in this topic.

#### - Solution viscosity

Diaz *et al.* (2006) explained that during the co-axial electrospinning process, sheath solution acts as a guide and surrounds the core forming co-axial jet at the tip of the Taylor cone. Therefore, viscosity of the sheath solution should be higher than the interfacial tension between two solutions [38]. On the one hand, Yu *et al.* (2004) reported that the viscosity of the sheath fluid is critical and the selected sheath polymer-solvent system should be electrospinnable by itself. Furthermore, since the formation of core structure is due to the shear stress generated from the sheath fluid, the viscosity of the core solution is not critical, and the selected core material-solvent system is not necessary to be electrospinnable. Yu *et al.* confirmed the findings by showing the TEM image (Figure 2.6) of electrospun silk/poly(ethylene oxide) core-sheath fiber, in which the core material, i.e., silk, is hard to process using conventional electrospinning [39].

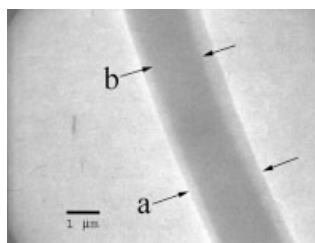


Figure 2.6 TEM image of electrospun silk/ poly(ethylene oxide) core-sheath fiber of Yu *et al* [39].

- Solution concentration

Zhang *et al.* (2004) experimented the effect of the concentrations on the morphology of a gelatin core and poly ( $\epsilon$ -caprolactone) shell nanofibers. It was found that an increased concentration of core solution would increase the diameter size of the fibers because of the increasing amount of material in the electrospinning jet [40]. This result is shown in Figure 2.7.

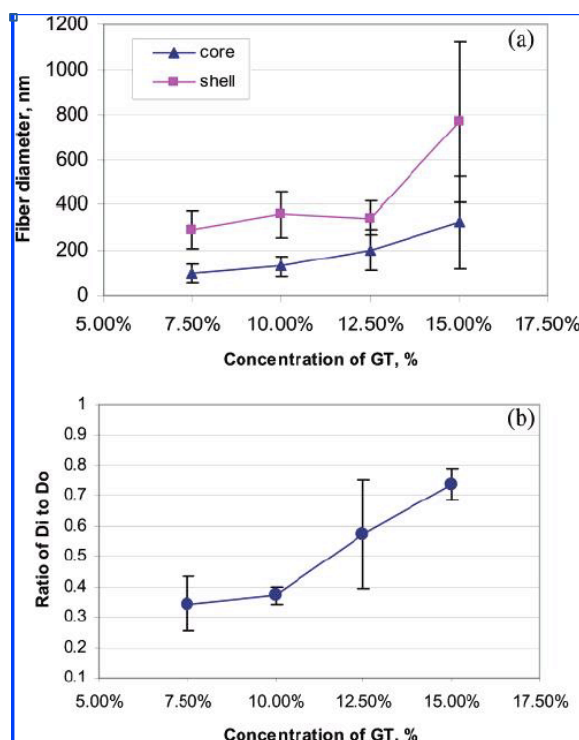


Figure 2.7 Effect of core solution concentration on the fiber diameter [40].

Similarly, He *et al.* (2004) observed an increase in the overall fiber diameter when higher sheath concentration was used in the co-axial electrospinning of tetracycline hydrochloride core and poly (L-lactic acid) [41].

- Solvent/solution miscibility and incompatibility

As the interaction between core material and sheath material is the important factor that has to be considered before choosing materials for co-axial

electrospinning, there are some criteria for choosing core and sheath materials. For electrospinning system, the solvents should not precipitate polymer when two solutions contact with each other at the tip of the nozzle. Regarding the miscibility of core solution and sheath solution, the opinions of different researchers diverge on this issue. Sun *et al.* (2003) proposed that the diffusion between the boundary of core solution and sheath solution would take longer time than the time that compound jet of solutions used for traveling to the collector. Thus, no mixing occurs at the boundary of core and sheath parts. They experimented co-axial electrospinning by using the solution of poly(ethylene oxide), water and ethanol in each core and sheath material with different concentration in core and sheath parts. Their result is shown in Figure 2.8(a), which can be seen in core-sheath structure [42]. This assumption was agreed by Yu *et al.* (2004), who experimented on Pani/PAN co-axial fiber fabrication using water as solvent in both core and sheath solution that makes core and sheath solution miscible. In this case, the product can still be seen as core-sheath structure as shown in Figure 2.8(b). They concluded that same solvent would reduce the interfacial tension between core and sheath solution, resulting in smooth interface of core and sheath parts [39].

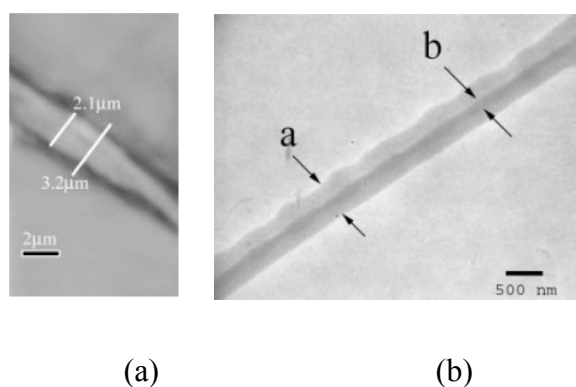


Figure 2.8 TEM images of miscible core solution and sheath solution

- (a): core and shell polymer solution of different concentration PEO in ethanol/water
- (b): Pani/PVP fiber using same water solvent

Li and Xia (2004) reported that the mixing between two miscible solutions could be occurred. They experimented on fabrication of co-axial fibers of two materials those are not dissolved together. By using mineral oil as a core material and  $\text{Ti}(\text{OiPr}_4)/\text{PVP}$  as a sheath material, they could get hollow fiber after removing mineral oil. After that, they used the solution of PVP in ethanol that can be dissolved in the sheath solution instead of mineral oil. After PVP removal by calcination, the fibers were not in hollow form as shown in Figure 2.9 [34]. Furthermore, Li and Xia had studied the fabrication of co-axial fibers using polystyrene in DMF/THF solution as a core solution and  $\text{Ti}(\text{OiPr}_4)/\text{PVP}$  in ethanol as a sheath solution. The results showed that the porous fiber could be obtained from this experiment (Figure 2.9). Therefore, they concluded that mixing could be occurred in co-axial electrospinning process in which two solutions are miscible.

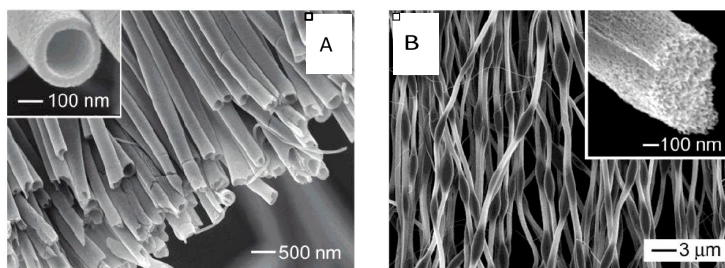


Figure 2.9 TEM images of Li and Xia research hollow fiber from mineral oil core solution and  $\text{Ti}(\text{OiPr}_4)/\text{PVP}$  sheath solution (A), and porous fiber from miscible PS/DMF/THF core solution in  $\text{Ti}(\text{OiPr}_4)/\text{PVP}$  sheath solution (B).

### *ii) Process parameters*

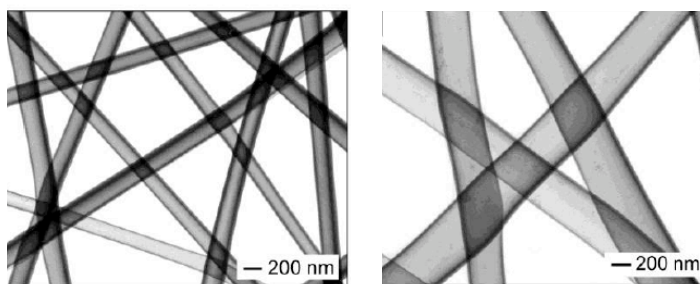
There are many parameters that can be adjusted in the co-axial electrospinning process for producing core-sheath fiber.

#### *- Applied electrical potential*

In co-axial electrospinning process, high potential would be applied to the solutions. The change of potential applied affected the fiber morphology. In the study of Li and Xia, who fabricated hollow fiber of  $\text{Ti}(\text{OiPr}_4)/\text{PVP}$  as explained earlier, they

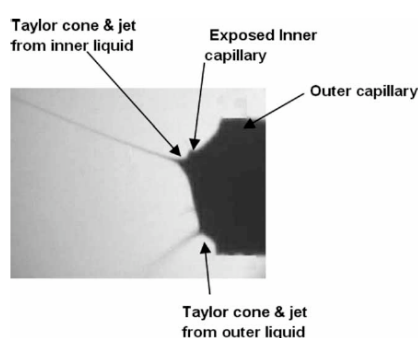
reported that both the inner and outer diameters of the fibers decreased upon the increase in strength of the electric field as shown in Figure 2.10(a-b) [34].

Gupta *et al.* (2008) proposed that there is a suitable range of the applied potential in each co-axial electrospinning system. The stable compound Taylor cone can only be obtained in this range. If the applied potential is too low, an electric force will not be enough to distort fluid into a conical shape. When an applied potential is too high, the jet will be split into small jets resulting in no core-sheath structure formed. It was confirmed by their experiments of producing polycaprolactone core and gelatin sheath fibers, in which the electrospinning could take place only under the voltage as small as 1 kV. When applied electrical potential was higher than 1 kV, the jet split into many small jets as shown in Figure 2.10 (c) [35].



(a)

(b)



(c)

Figure 2.10 TEM images of Li and Xia 's hollow fiber of Ti(OiPr<sub>4</sub>)/PVP under higher voltage (a) and lower voltage (b), split jets from PCL core and gelatin sheath solution of Gupta *et al.*, when the voltage is too high (c).

- Solution flow rate

Two fluids are fed into a co-axial nozzle in the co-axial electrospinning process. Thus the flow rates of core fluid and sheath fluid should be adjusted for making the stable compound Taylor cone.

For the effect of core flow rate, Diaz *et al.* (2004) concluded that when the sheath flow rate and other parameters were fixed, if the core flow rate is too high, the mixing of the core fluid and the sheath fluid will occur. In other words, the sheath may fail to completely encapsulate the fast moving core to form the compound cone as shown in Figure 2.11 [38].

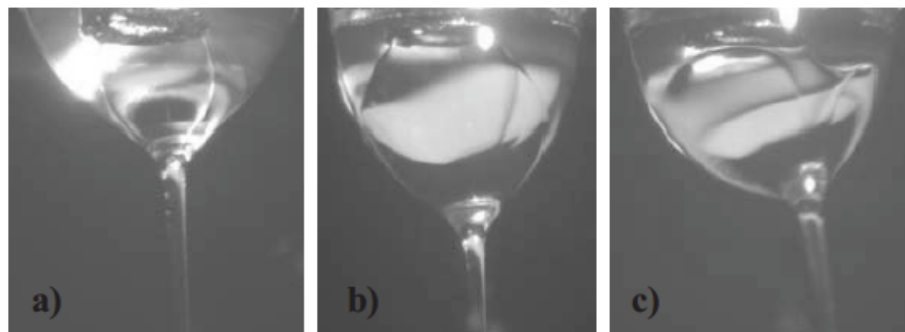


Figure 2.11 Compound cone formed when the sheath flow rate is constant and while the core flow is increased from a), b) and c) respectively [38].

Both core and sheath solution flow rates are directly control the dimension of the fiber product in electrospinning because the amounts of materials are changed when the flow rates are changed.

- Distance between the tip of the nozzle to collector

The distance from tip of the nozzle to the collector can be called “working distance”, which should be in a suitable range in each electrospinning system similarly to the electrical potential applied. The working distance directly affects the strength of electric field in electrospinning process. Therefore, the decrease in



working distance, which means higher electric field strength, could result in smaller diameter of the fibers.

## CHAPTER III

### EXPERIMENT

#### 3.1 Chemicals

1. Titanium (IV) isopropoxide (TTIP) was purchased from Wako Pure Chemical Industries, Ltd. and used as received.

2. Polyvinylpyrrolidone (PVP),  $M_w \sim 1,300,000$ , was purchased from Sigma-Aldrich Chemical Company and used as received.

3. Polyacrylonitrile (PAN),  $M_w \sim 86,200$ , was purchased from Sigma-Aldrich Chemical Company and used as received.

4. N,N'-dimethylformamide (DMF) was purchased from Kanto Chemical Company and used as received.

5. Acetic acid was purchased from Kanto Chemical Company and used as received.

#### 3.2 Electrospinning Apparatus

The schematic of the electrospinning apparatus is shown in Figure 3.1. The components of the apparatus and their functions are described as follows.

- A high voltage power supply (R6243, DC voltage current source/monitor, Advantest, Japan) was used to generate either positive or negative DC voltage up to 30 kV, with very low electrical current.
- A co-axial copper nozzle of which the core diameter is equal to that of the stainless needle (gauge number 22, the outer diameter of 0.7 mm) and outer diameter of the sheath is 1.5 mm will be attached to two syringes for producing co-axial fiber.
- Two 10 ml syringes were used as containers for electrospinning solutions. The syringes are built by plastic structure and set in horizontal orientation.
- Aluminum foil was considered to be a ground collector

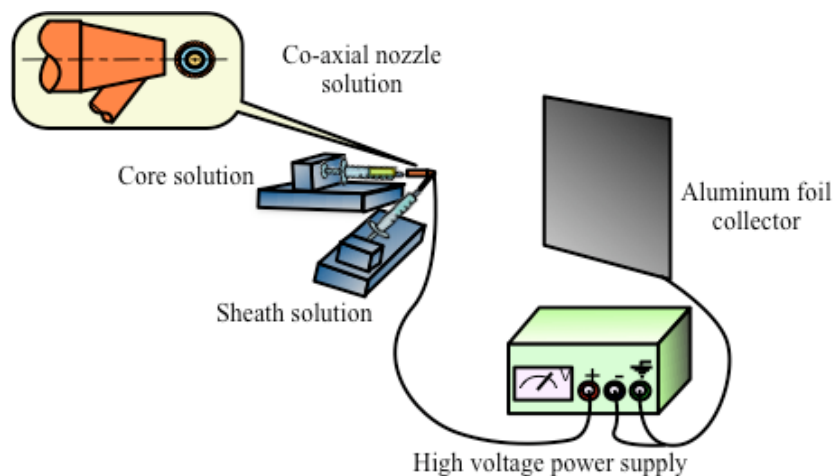


Figure 3.1 Schematic of an electrospinning setup.

### 3.3 Experimental Procedures

#### 3.3.1 Preparation of electrospinning solutions

##### *Preparation of PAN/PVP co-axial electrospinning solution*

PAN solution was prepared by dissolving polyacrylonitrile in *n,n'*-dimethylformamide at 60°C and will be constantly stirred for 1 h, while PVP solution was prepared by dissolving polyvinylpyrrolidone in *n,n'*-dimethylformamide at room temperature. In this study, the concentration of each solution was varied to investigate the effect of the concentration.

##### *Preparation of PAN-TiO<sub>2</sub>/PVP co-axial electrospinning solution*

The core solution of PAN was prepared in same manner as previous described. The sheath solution was prepared by combining PVP, acetic acid, DMF and titania precursor i.e., TTIP. Firstly, dissolving 2.5 g of PVP in 20 ml of DMF for preparing PVP solution. Then, the titania-precursor solution was prepared in another vial by stirring 3 ml of TTIP together with 6 ml DMF and 6 ml acetic acid for 15 min. The precursor solution was slowly added into the PVP solution and stirred for 70 min to obtain the sheath solution.

### **3.3.2 Co-axial electrospinning process**

Each electrospinning solution was instantly filled into each plastic syringe, which was furnished into the co-axial nozzle. The syringe which contains PAN solution was connected to the core of the nozzle and another syringe connected to the shell of the nozzle contained PVP solution for producing PAN-PVP core-sheath fibers. On the other case, the syringe connected to shell of the nozzle contained TiO<sub>2</sub>/PVP solution for producing PAN-TiO<sub>2</sub>/PVP core-sheath fibers. The emitting electrode from the power supply was attached to the nozzle. The grounding electrode from the same power supply was attached to a piece of aluminum foil, which was used as the collector plate and was placed in front of the tip of the nozzle. The distance between the tip of the nozzle and the collector would be investigated. Upon the application of high voltage across the nozzle and the collector in the range of 20-22 kV, which will also be investigated, a fluid jet will be ejected from the nozzle. As the jet accelerated towards the collector, the solvent evaporated, leaving only ultrathin fibers on the collector. In addition, the fibers products were left for completely evaporation of solvent for 24 h.

### **3.3.3 Calcination of the PAN-TiO<sub>2</sub>/PVP core-sheath fibers**

The calcination of electrospun PAN-PVP/titania core-sheath nanofibers was performed in a box furnace. The temperature of the furnace was raised from room temperature to 450°C with heating rate at 5°C/min, then hold at this temperature for 2 h.

## **3.4 Characterizations of Products**

### **3.4.1 Scanning electron microscopy (SEM)**

Morphology of the obtained products was determined by using JEOL scanning electron microscopy model JSM-7600F and JSM-6400 at Ceramics Research Laboratory, Nagoya Institute of Technology, Japan and the Scientific and Technological Research Equipment Center (STREC), Chulalongkorn University,

respectively. Moreover, sizes of the products were then measured from the SEM micrographs.

In addition, the core-sheath structure of fibers were confirmed by using scanning transmission electron microscopy (STEM) and the composition of fibers was investigated by energy dispersive x-ray spectroscopy (EDX). STEM and EDX are accompanied with SEM at Ceramics Research Laboratory, Nagoya Institute of Technology, Japan.

#### **3.4.2 Transmission electron microscope (TEM)**

The core-sheath structures of the fibers were investigated by using JEOL transmission electron microscopy model JEM-2010 at Ceramics Research Laboratory, Nagoya Institute of Technology, Japan.

#### **3.4.3 Rheometer**

The viscosities of the solutions were measure by using cone and plate type of Thermo Scientific HAAKE RheoStress 6000 rheometer at Ceramics Research Laboratory, Nagoya Institute of Technology, Japan.

#### **3.4.4 Thermogravimetric analysis (TGA)**

The decomposition temperature and thermal behavior of the obtained products were studied by using thermogravimetric analysis on a Rigaku Thermoplus TG8120 at Ceramics Research Laboratory, Nagoya Institute of Technology, Japan and a Mettler-Toledo TGA/DSC1 STARe System at Center of Excellence in Particle and Technology Engineering laboratory, Chulalongkorn University. The samples were heated under the oxygen flow of 40 ml/h and the ramp rate of 10 °C/min.

#### **3.4.5 Fourier-transform infrared spectroscopy (FT-IR)**

A Fourier transform infrared spectrometer (Nicolet 6700) at Center of Excellence in Particle and Technology Engineering laboratory, Chulalongkorn University were used to investigate the functional group in the products. The samples

of the products were mixed with KBr in a ratio of sample to Kbr 1:100 before measurement.

#### **3.4.6 X-ray diffraction analysis (XRD)**

The crystalline phase was analyzed by x-ray diffraction. Rigaku Ultima IV diffractometer with  $\text{CuK}\alpha$  radiation was used for scanning the sample in the range of  $2\Theta = 20 - 60^\circ$ .

#### **3.4.7 Universal testing machine (UTM)**

The tensile strength of the fiber products was measured by Lloyd Universal Testing Machine, using at The Analytical and Testing Service Center, The Petroleum and Petrochemical Collage, Chulalongkorn University. The films of fiber products were cut into a dimension of  $1 \times 3 \text{ cm}^2$  in width and length, respectively. The thickness of the films is control by the electrospinning time of 5 h. The specimens were pulled by the load of 1 kg with the rate of 10 N/min while measuring.

## CHAPTER IV

### RESULTS AND DISCUSSION

In this chapter, the fiber products fabricated from the combination of sol-gel and electrospinning processes were analyzed. The core-sheath structure of the fibers was confirmed. The effects of preparation conditions and processing parameters on characteristic of the fibers were studied. Furthermore, effects of calcination process for PVP removal and titania crystallization were investigated. The last part of this chapter will investigate the flexibility of the PAN/TiO<sub>2</sub> co-axial fibers.

#### 4.1 Core-Sheath Structure Formation of PAN/PVP Fibers

According to the research objective, it is necessary to confirm that the core-sheath structure of PAN/titania(PVP) fibers could be obtained by the co-axial electrospinning process using PAN core solution and titania(PVP) sheath solution.

As noted in Chapter II, mixing could occur in co-axial electrospinning process of miscible core/sheath solutions. Therefore, PAN/PVP co-axial fibers were fabricated to test the ability to form the core-sheath structure from PAN core solution and PVP sheath solution, both of which are miscible. Moreover, effects of solution viscosities on the fiber morphology were also studied. As there is a range of suitable viscosity of the solution for producing fibers from the conventional electrospinning process. In the co-axial electrospinning, it is still not clear that the core solution and the sheath solution are necessary to be electrospun separately. In this research, the concentration of each solution that could produce the electrospinnable solutions were considered. Therefore, the starting concentration of PAN was in the range of around 8%wt, which could produce the PAN smooth fibers [43]. On the same way for PVP solution, the concentration that can produce uniform PVP fibers around 10wt%, while the measured viscosity is around 0.1 Pa.s [44]. SEM images in Figure 4.1 show that the smooth and uniform fibers could be fabricated only when the concentration of both solutions are in proper range. Beads are formed on the fibers when the PAN concentration is 6 %wt. On the other hand, when the concentration of PAN is

increased to 10 %wt, the fibers formed are less uniform in size. The proper concentration of PAN was found to be 8 %wt.

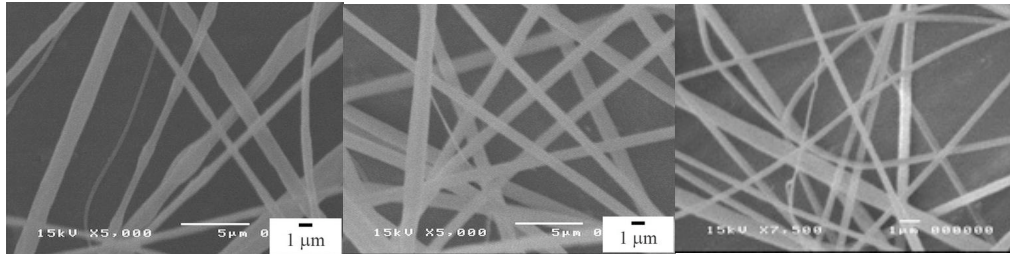


Figure 4.1 SEM images of products of PAN solution and PVP solution whereas the concentrations of PVP and PAN solutions are 10/6 (a), 10/8 (b), and 10/10 (c) %wt/%wt, respectively.

To study the effect of PVP concentration and viscosity, the fibers were prepared from the core solution of 8wt% PAN in DMF, together with the sheath solution of PVP at 10wt%, 13wt% and 15wt% in the DMF as well. The increase in the concentration of the sheath solution results in the increase in solution viscosity as shown in Figure 4.2. Nevertheless, both solutions are electrospinnable under an electric potential of 22 kV applied across the working distance of 22 cm

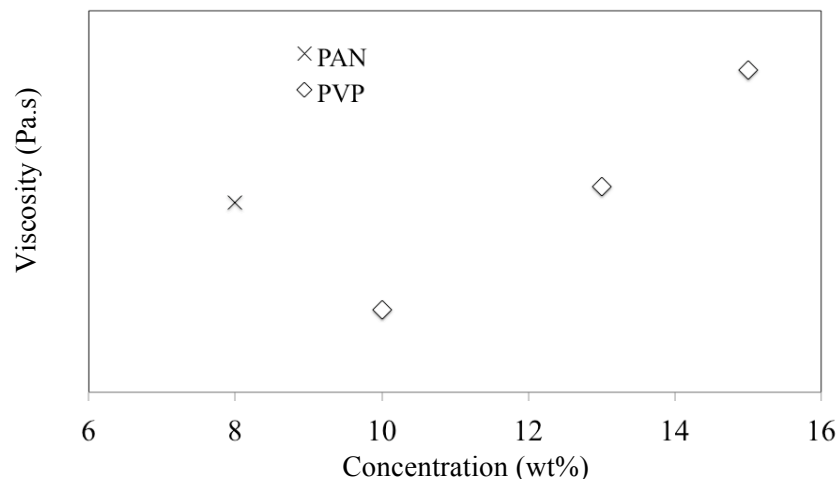


Figure 4.2 Viscosity of PVP and PAN solutions at different concentration.



The co-axial electrospun fibers were observed by TEM micrographs as shown in Figure 4.3, which confirm that the obtained products are indeed core-sheath nanofibers. The boundary between core material and sheath material can be seen from these TEM micrographs.

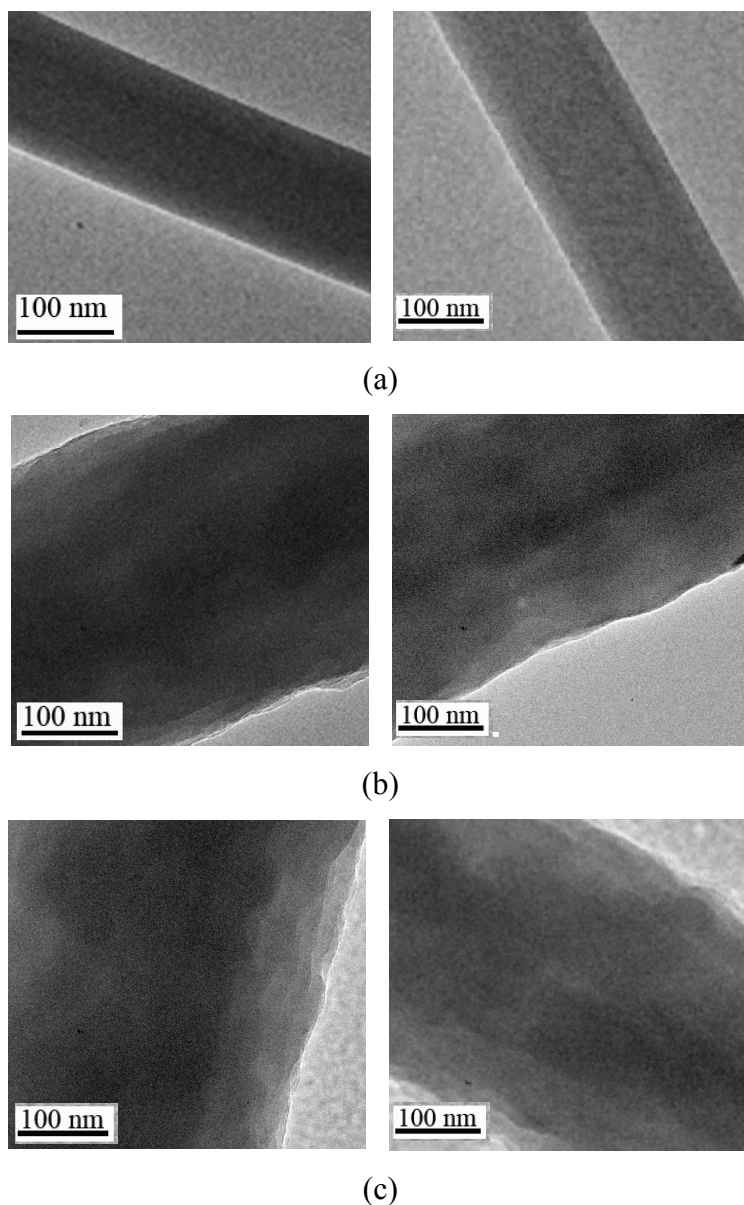


Figure 4.3 TEM micrographs of products obtained from co-axial electrospinning of PAN (core) solution and PVP (sheath) solution using applied potential of 22 kV and the distance from nozzle to collector of 22 cm, whereas the concentrations of PAN and PVP solutions are 8/10 (a), 8/13 (b), and 8/15 (c) wt%/wt%, respectively.

Miscibility of core and sheath solution is one of parameters affecting core/sheath structure of the fibers in Chapter II. In this research, even though it is possible to find the mixing between core and sheath solution during electrospinning, it is confirmed that miscible PAN core and PVP sheath solutions could be used for making core-sheath fibers. This can be explained by the fact that the diffusion at the boundary of core solution and sheath solution would take longer time than the time that compound jet of solutions used for traveling to the collector. Thus, no mixing occurs at the boundary of core and sheath parts [42]. This hypothesis have been proved by some researches such as, in the preparation of miscible poly-L-lactide core and poly-DL-lactide co-axial fibers[45], in the preparation of co-axial fiber using  $\text{Ti}(\text{OiPr}_4)/\text{PVP}$  in ethanol as a sheath solution and PVP in ethanol that can be dissolved in the sheath solution as a core solution.

Considering the effects of viscosities on morphology of the co-axial fibers, when the viscosity of the sheath solution is increased higher than that of the core solution, the outer surface of the fibers becomes rough and the core-sheath structure is less defined. This can be explained by the conical flow of the solution from Taylor's cone, which develops the stress upon the interface between the core solution and the sheath solution. High viscosity of the sheath solution would produce large droplet at the end of the nozzle, which subsequently becomes conical shape after the electric potential is applied. As the result, high shear stress is introduced to the core/sheath interface leading to the mixing of the core/sheath solutions. It can be described that when high voltage is applied, the compound droplet is stretched to flow conically to form compound cone, in which shear stress developed in the sheath solution will exert on the core solution at the core-sheath interface. Large droplet yields larger angle of the Taylor's cone, which develops higher shear stress in sheath solution as well as at the interface of core-sheath.

It can be concluded that the suitable value of concentration of PAN solution for this co-axial system is 8wt%, which provide the viscosity of around 0.2 Pa.s. The suitable viscosity of sheath solution of PVP is confirmed to be around 0.1 wt% as same as the preparation of PVP pure fibers. These viscosity values of core and sheath solutions were then chosen to use in PAN/titania(PVP) fabrication.

In addition, it can be seen from Table 4.1 that the sheath solution concentration has an influence on the size of the co-axial fibers. The increase in concentration of the sheath solution results in the increase in fiber size since the amount of sheath material is increased [41]. Hence, the increase in interaction between molecules of the sheath material, is increased, results in sheath thickness increased. Since the concentration of the core solution was kept constant, the major cause of the increase in the size of the fibers is related to that the sheath thickness increased, which is also confirmed by the decrease in core diameter to sheath thickness ratio.

**Table 4.1** Ratio of the core diameter to the sheath thickness of fibers produced using different concentrations of PVP solution.

Concentration of PVP sheath solution (wt%)	Average fiber diameter (nm)	Average sheath thickness (nm)	Core diameter / Sheath thickness
10	130	26	3.2
13	340	84	2.1
15	370	97	1.9

#### 4.2 Co-axial Electrospinning of PAN/TiO<sub>2</sub>(PVP) Fibers

The preparation of PAN/titania(PVP) co-axial fibers is similar to that of PAN/PVP co-axial fibers. PAN (8wt%) in DMF solution was used as the core solution, while the sheath solution was changed from PVP solution to be the solution of titania precursor, i.e., mixture of TTIP, acetic acid and DMF and PVP. Viscosity of the sheath solution was chosen from the suitable value studied in the fabrication of PAN/PVP co-axial fibers.

The viscosity of the solution of titania precursor was adjusted by varying concentration of PVP. As stated in Topic 3.3.1, PVP was dissolved in DMF before adding to the solution of TTIP, acetic acid and DMF. Different concentration of PVP

solution before mixing with titania solution were used for preparing different solution viscosities.

Figure 4.4 shows the viscosity curve of titania solution used in preparation of PAN/titania(PVP) co-axial fibers. It can be seen that the sheath solution prepared from 12wt% of PVP solution provides almost same value of viscosity as 10wt% PVP sheath solution, which has proved to be proper for the fabrication of PAN/PVP co-axial fibers.

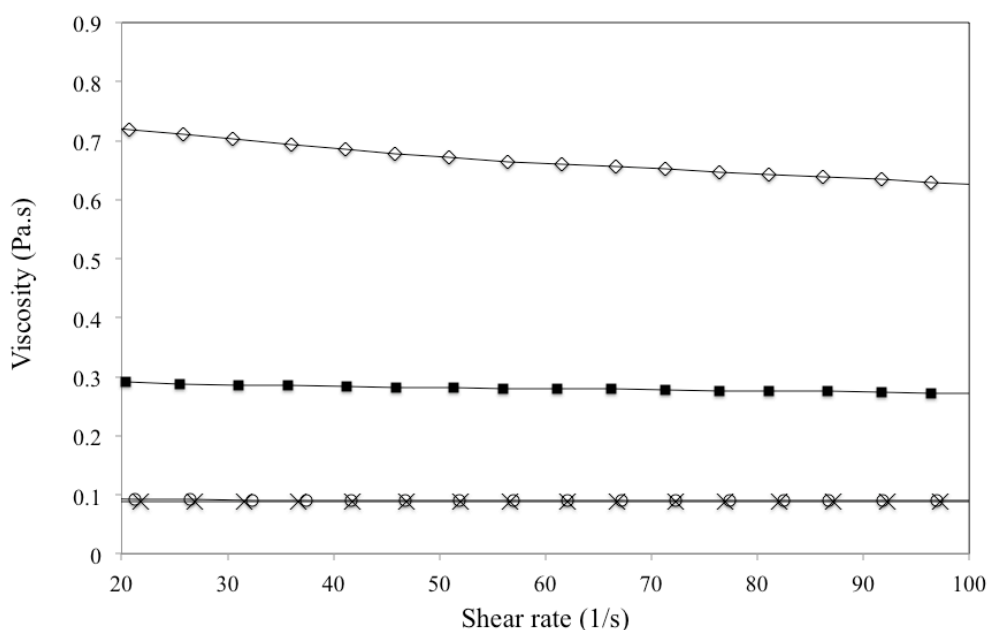


Figure 4.4 Viscosity curve of titania precursor solution prepared from PVP solution concentration of 24wt% ( $\diamond$ ), 18wt% ( $\blacksquare$ ) and 12wt% ( $\circ$ ) compared with that of 10wt% PVP solution used as sheath solution in PAN/PVP co-axial electrospinning ( $\times$ ).

To confirm that the chosen viscosity of the sheath solution is suitable, Figure 4.5 shows the TEM image of the co-axial PAN/titania(PVP) fibers. The core sheath structure can be defined clearly, even though the sheath part is not smooth as the PAN/PVP fibers. This may consider as the effect of titania precursor solution mixed with PVP solution. Furthermore, size of PAN/titania(PVP) fibers, which was prepared using solution with similar viscosities as that used to produce PAN/PVP fibers, is larger than that of PAN/PVP fibers. This result can be described that the titania

precursor solution added in the sheath solution gives higher amount of material in solution, which makes fiber to become larger. Additionally, size of the PAN core is relatively close to that observed in PAN/PVP co-axial fiber. Therefore, a change in the sheath solution has no effect on PAN core as long as the same concentration of the core solution is used.

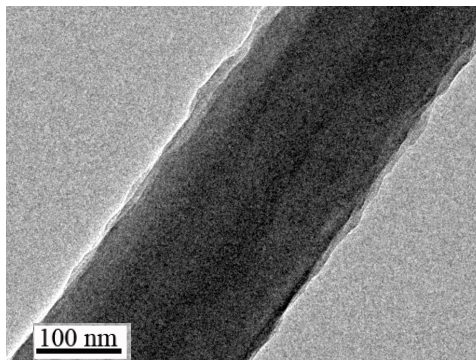


Figure 4.5 TEM of PAN/titania(PVP) co-axial electrospun fiber.

After the suitable condition for the solution preparation was selected for co-axial electrospinning process, the effects of processing parameters on the morphology of PAN/titania(PVP) as-spun co-axial fibers were studied and reported.

#### **4.2.1 Effects of solution flow rate**

During co-axial electrospinning process, syringe pumps were used to control the solution flow rates, which would affect the electrospun fiber morphology. The effect of the flow rates of the solutions in the co-axial electrospinning process is shown in STEM images in Figure 4.6. The STEM operated in a very similar way to SEM. By using a fine, highly focused beam of electrons scanned over a thin specimen. Electrons that pass through the sample can be collected to produce a variety of transmission images, but, as with the TEM, backscattered electrons and X-rays are also produced. Secondary electrons (SE) are also produced, giving yet another imaging mode. One of the most common ways of carrying out STEM has been to add transmission detectors to an SEM. Therefore, the light zone in the STEM images is not an effect from the charge since only transmitted electron moving through the specimen is detected.

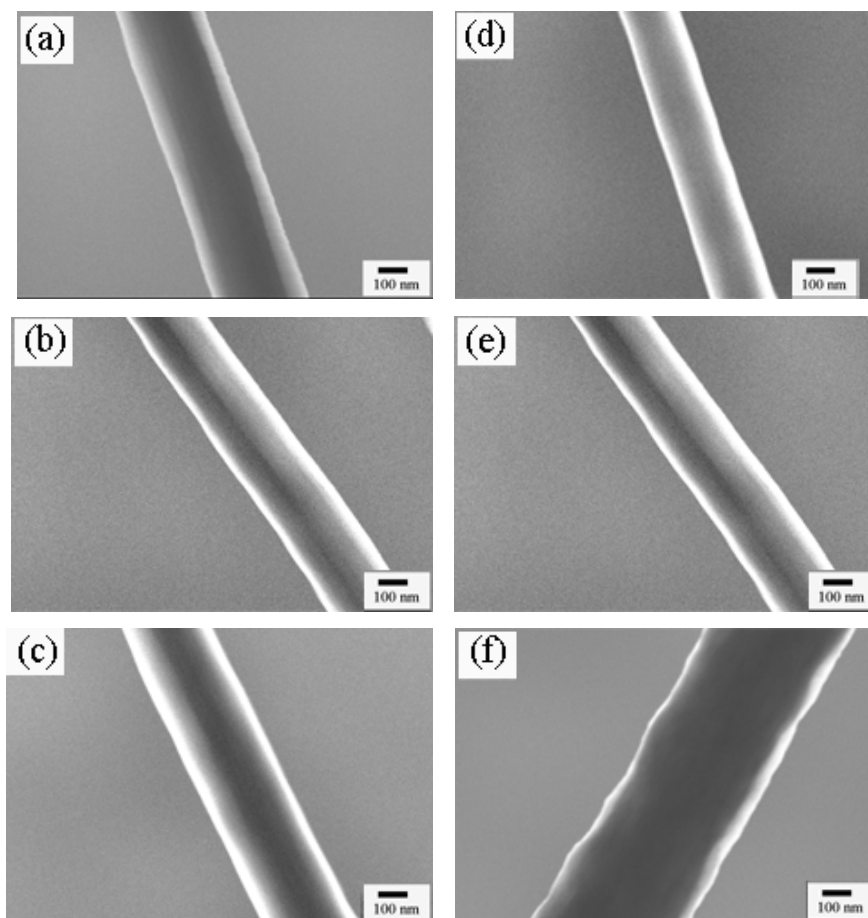


Figure 4.6 STEM images of products obtained from co-axial electrospinning of PAN solution and PVP/titania solution using applied potential of 22 kV and the distance from nozzle to collector of 22 cm, whereas the flow rate of PAN and PVP/titania solutions are 1.2/0.9 (a), 1.2/1.2 (b), 1.2/1.5 (c), 0.9/1.2 (d), 1.2/1.2 (e) and 1.5/1.2 (f) (ml/h)/(ml/h), respectively.

From Figure 4.6(a-c), it can be seen that the increased flow rate of the sheath solution, which consequently increases the shear stress in the solution, results in the rough surface and the mixing of two solutions in similar manner as the effect of viscosity previously discussed. As explained in the previous topic, when the electric potential is applied, large droplet of the sheath solution could develop high stress in the sheath solution at the interface between the core solution and the sheath solution, which is shown in Figure 4.7. Size of the droplet is not only controlled by the

viscosity of the solution, but also the flow rate of the solutions. The increase in the flow rate results in the increase in droplet size due to higher amount of material supplied.

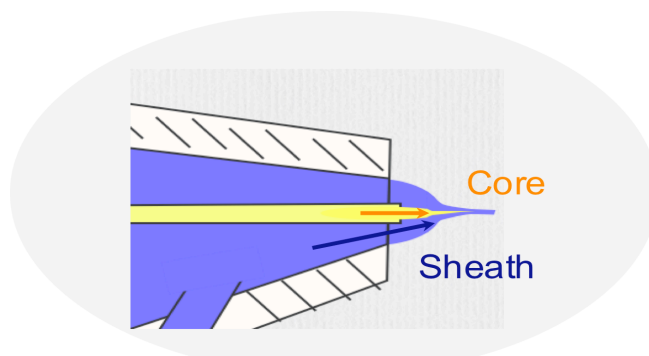


Figure 4.7 Taylor cone at the tip of co-axial nozzle when electric potential applied.

In addition, it can be seen from Figure 4.6(d-f) that the increase in the flow rate of the core solution, which increases the amount of supplied core material, results in the increase in the diameter of the fibers.

#### 4.2.2 Effects of electric potential

Another important factor that affects morphology of the electrospun fiber is the applied electric potential. In electrospinning system, stable jet of the spinning solution ejected from the Taylor's cone could be formed only when the applied potential is in suitable range.

The effect of the electric potential applied for the co-axial electrospinning depends on type of fluids used and the distance between the tip of the nozzle and the collector, i.e., working distance. Consider the PAN-PVP/titania fibers fabricated, the electric potential of 20 and 21 kV could produce the fibers as shown in Figure 4.8(a) and 4.8(b) respectively. However, the fibers are not uniform in size due to the unstable jet formed during the electrospinning process. The proper electric potential for this system was found to be 22 kV, as shown in Figure 4.8(c), in which uniform fibers without beads were produced. Distributions of the diameter of fibers are shown in Figure 4.9 and 4.10.

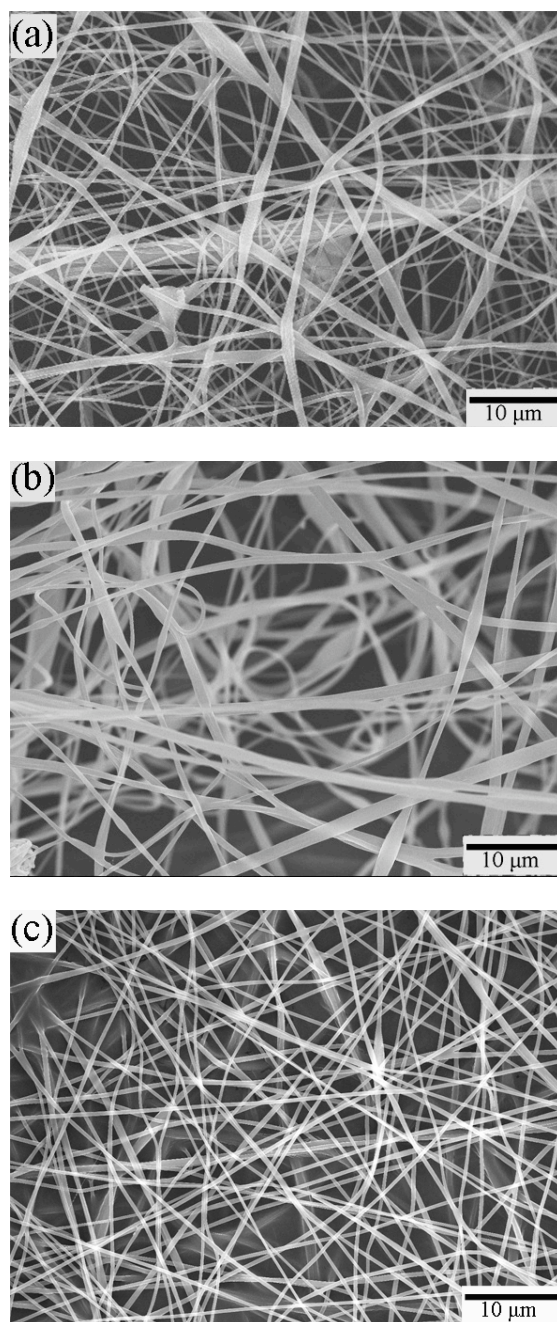


Figure 4.8 SEM images of the products obtained from the co-axial electrospinning of PAN solution and PVP/titania solution with the tip-to-collector distance of 22 cm and the applied electric voltage are 20 kV (a), 21 kV (b), 22 kV (c) respectively.



Generally, the average diameter of the fibers is decreased when the applied electric potential is increased. It should be noted that the change in diameter of the fibers when the applied potential is adjusted is not clear due to the presence of the beads. The decrease in size of diameter the can be explained by the fact that an increased potential heightened the electric repulsive force on the fluid jet, which consequently causes greater stretching of the solution due to the greater columbic forces in the jet as well as a strong electric field and leads to the reduction in the fiber diameter [46].

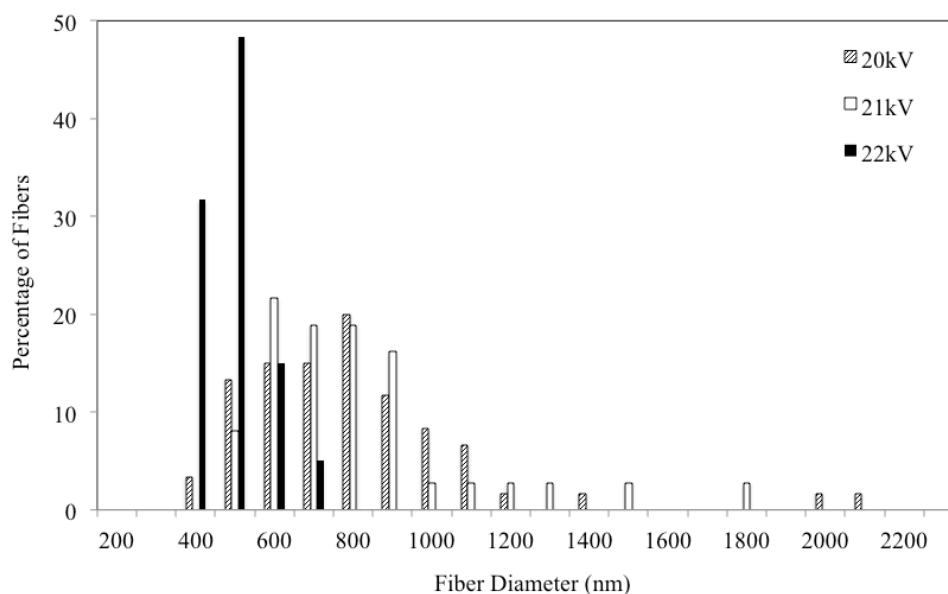


Figure 4.9 Histogram of diameter size distributions of PAN/TiO<sub>2</sub>(PVP) co-axial fibers obtained from the co-axial electrospinning of PAN solution and PVP/titania solution with the tip-to-collector distance of 22 cm and the applied electric voltage 20 kV, 21 kV and 22 kV respectively.

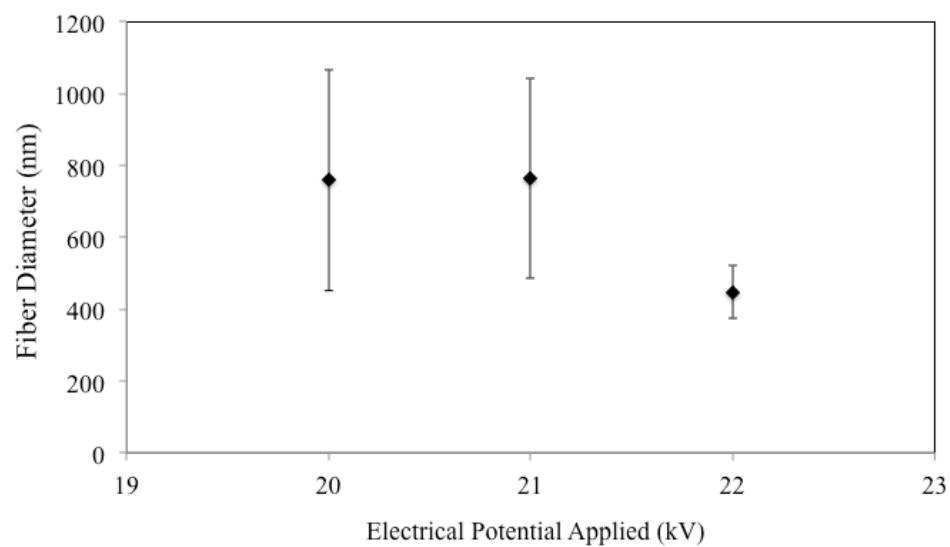


Figure 4.10 Average diameter of PAN/TiO<sub>2</sub>(PVP) co-axial fibers obtained from the co-axial electrospinning of PAN solution and PVP/titania solution with the tip-to-collector distance of 22 cm and the applied electric voltage 20 kV, 21 kV and 22 kV respectively. The error bar shows standard deviation of the data.

### 4.3 Core-Sheath Structure of PAN/Titania Fibers

To obtain PAN/titania co-axial fibers, calcination of as-spun PAN/PVP(titania) co-axial fiber is necessary. The temperature of the calcination should be high enough to remove PVP polymer in the sheath part of the fibers as well as to crystallize titania to anatase form. The characterizations of the co-axial fiber will be explained in this topic.

#### 4.3.1 Thermal Gravimetric Analysis (TGA)

The temperature of calcination was firstly determined by thermal gravimetric analysis result of the PAN/PVP(titania) co-axial fibers. Figure 4.11 shows the TGA thermogram of PAN/PVP(titania) as-spun co-axial fibers being heated up to temperature of 800 °C under oxygen gas.

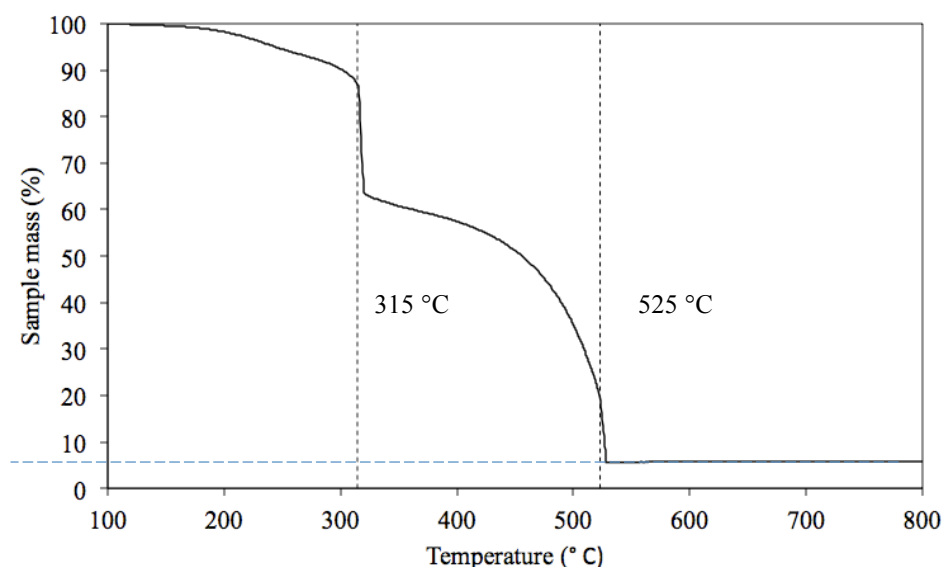


Figure 4.11 TGA curve of PAN/PVP(titania) co-axial electrospun fibers.

The result shows the sample mass loss in two steps, which is similar to the degradation of PAN pure fiber as shown in Figure 4.12. The first decrease of mass in both co-axial fibers and PAN pure fibers is at temperature around 315 °C, which is around the beginning of degradation temperature of PVP. Therefore, the mass decrease at first step of co-axial fibers is expected to be the effects of the degradation of PVP and stabilization of PAN fibers.

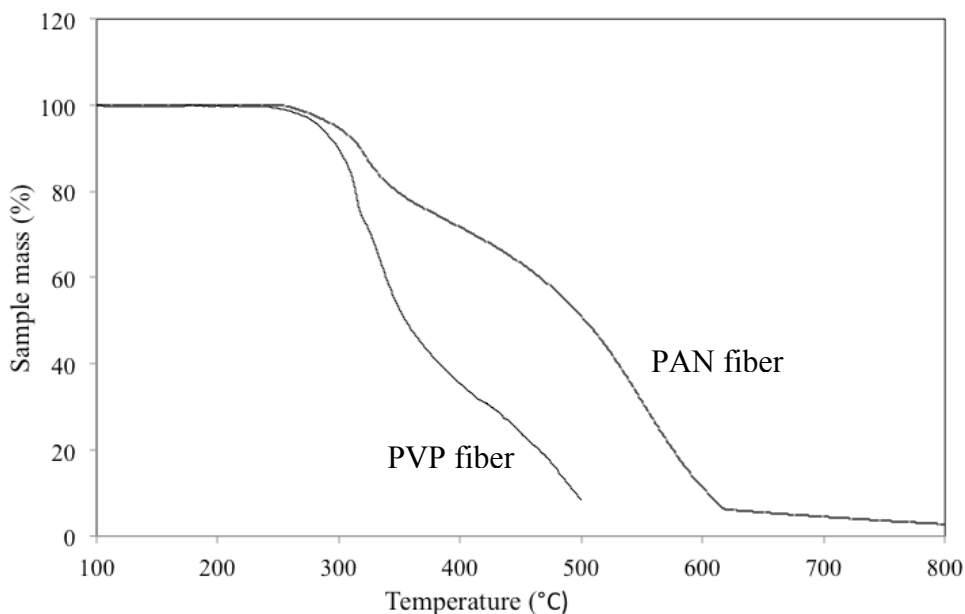


Figure 4.12 TGA curve of PAN and PVP electrospun fiber.

The stabilization of PAN normally occurs when PAN is heated in air at around 300 °C. In this process, some exothermic chemical reactions of cyclization oxidation and dehydrogenation occur. The rate of weight loss in the first step is quite rapid due to the dehydrogenation of PAN. Figure 4.11 shows that the decrease of mass in the first step of co-axial fibers is around 40 wt%, which is larger than the summation of mass loss of each PAN and PVP calculated separately from TGA thermogram of pure polymer fibers. It can be implied that titania has influenced the dehydrogenation of some compound [47].

Besides, Figure 4.13 shows that there is heat flow from exothermic reaction at the same temperature, which conforms to the dehydrogenation of PAN and the decomposition of pure PVP fiber normally decomposing at temperature around 320 °C as shown in Figure 4.12.

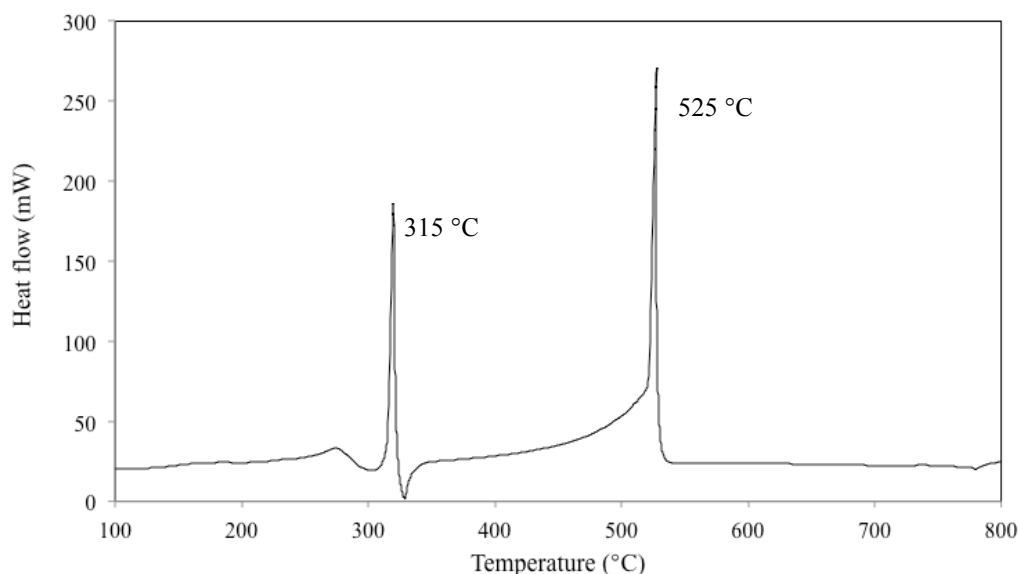


Figure 4.13 DSC curve of PAN/PVP(titania) co-axial electrospun fibers.

The second mass decrease is not rapid as in the first step, hence the mass of fibers is slowly decreased when they are heated up above 320 °C. This can be explained by the partial evaporation of small compound, such as  $\text{NH}_3$  and  $\text{HCN}$  from the fragmentation of polymers. At temperature of 525 °C, it is expected to be the temperature of the complete degradation of PAN and PVP in fibers. In this temperature, mass of the fibers decreases rapidly and the DSC curve confirms that the exothermic reaction occurs.

Considering the amount of titania in co-axial fibers, the TGA curve in Figure 4.11 shows the amount of titania remaining in fibers. It can be seen that the mass of the co-axial fibers is constant while being heated up at the temperature in the range of 600 °C to 800 °C. At 800 °C, all carbonaceous materials including PAN core should be totally decomposed by reacting with oxygen gas. The temperature of complete degradation of PAN was found to be around 780 °C according to the study of Korobeinyk, *et al* [48]. Thus, only titania remains after heating. The amount of titania determined by TGA curve is found to be around 7 wt% of the fibers, which is less than the calculated value of 10 wt%. It might be affected from the non-uniformity of titania in the fibers.

For the calcination temperature, as seen in TGA curve of pure PVP fiber, although PVP is decomposed at the temperature of 320 °C, it still remains its mass around 50%. Consider the TG curve of the co-axial fiber, mass of fibers decreased slowly after the first step of mass lost referring to the decrease of PVP, while PAN curve is almost constant. The chosen temperature for calcination was found to be 450 °C since after 450 °C the second decrease of PAN is started again, which can be seen from both TG curves of co-axial fiber and PAN fibers.

#### 4.3.2 Effect of calcination on the co-axial fibers

As a result from TGA, the calcination temperature was chosen to be 450 °C, which is high enough for removing PVP polymer from the sheath part of co-axial fibers and not too high to degrade most part of PAN core. After calcination of the electrospun fibers at 450 °C for 2 h, the products remain in fiber form as shown in Figure 4.14(b) and still retains its flexibility. The flexibility of the calcined fibers implies for the presence of the PAN core.

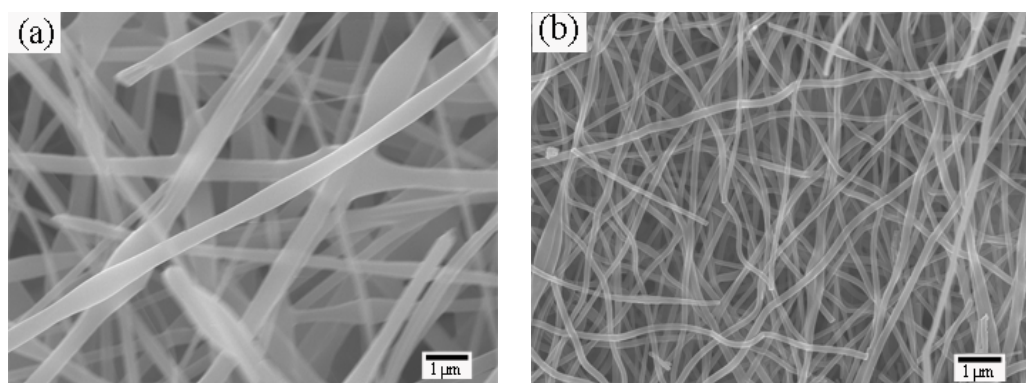


Figure 4.14 SEM images of the products obtained from the co-axial electrospinning of PAN solution and PVP/titania solution with the tip-to-collector distance of 22 cm and the applied electric voltage of 22 kV, before (a) and after calcination at 450 °C for 2 h (b).

Figure 4.15 shows size distribution of co-axial fibers of PAN/PVP(titania) and PAN/titania. The average diameter of the fibers decreases from 370 nm to 160 nm after calcination, which could be explained by the removal of PVP in the sheath structure of the fibers by the calcination.

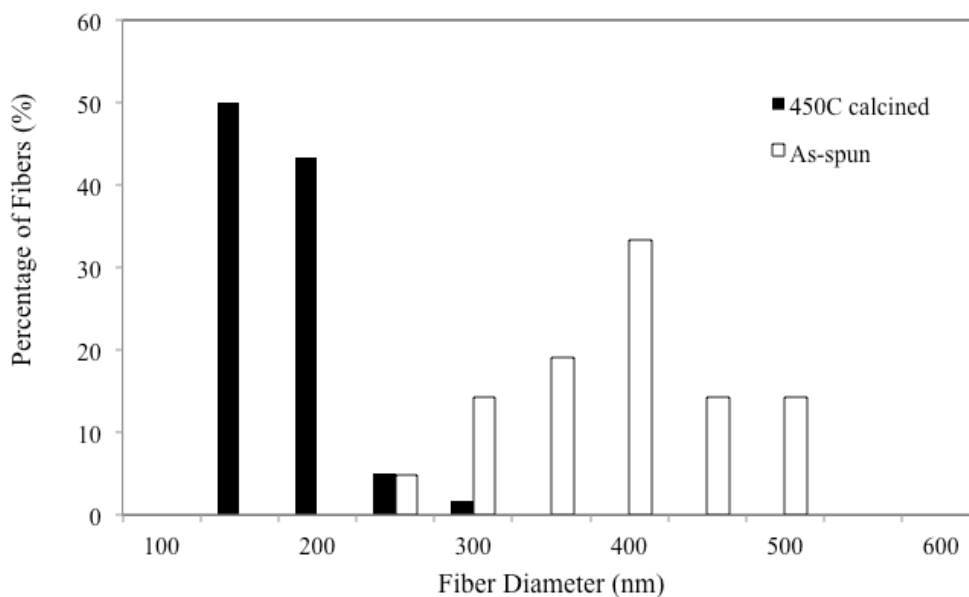


Figure 4.16 Histogram of diameter size distribution of as-spun PAN/TiO<sub>2</sub>(PVP) co-axial fibers and PAN/TiO<sub>2</sub> co-axial fibers after calcination at 450 °C for 2 h.

According to the TGA analysis, when the calcination temperature is increased, mass of the obtained fiber decreases. The morphology of the products after being calcined at different calcination temperature was investigated to confirm the fiber structure during calcination process.

Figure 4.16 shows SEM images of co-axial fibers of PAN/PVP(titania) after being calcined at 300 °C, 450 °C and 800 °C respectively. It can be seen from the figure that all obtained fibers remain in fiber form. The as-spun co-axial fibers and the fibers after calcination at temperature of 300 °C shown in Figure 4.16(a) and 4.16(b), respectively, are similar in size and morphology. This supports the TGA result that no polymer loss occurs below the temperature of 315 °C. While heating up to 450 °C, the fibers lost their mass according to the removal of PVP, which also results in the

decrease in diameter of fibers. Finally, when the calcination temperature is raised to 800 °C, both of PAN polymer and PVP polymer are removed of the fibers. Figure 4.16(d) shows the titania fibers with rough surface and having a chain-like structure, which could be affected from the removal of PAN core from the fibers.

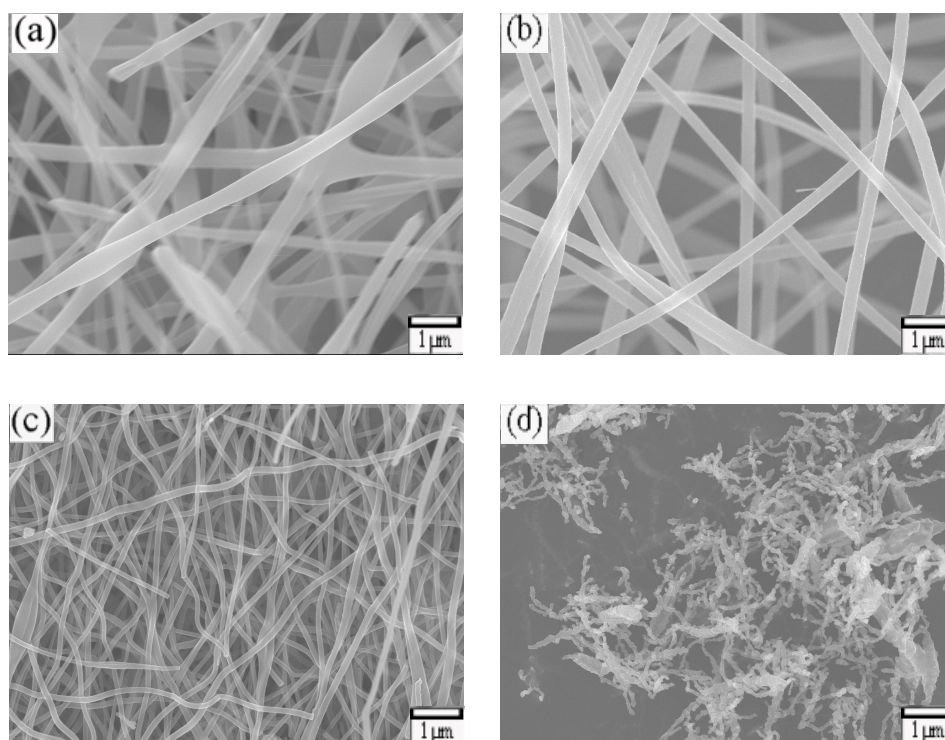


Figure 4.16 SEM images of the fibers obtained from the calcination of co-axial electrospun fiber of PAN solution and PVP/titania solution with the tip-to-collector distance of 22 cm and the applied electric voltage of 22 kV, before (a) and after calcination at 300 °C (b), 450 °C (c) and 800 °C (d) respectively.

Furthermore, it can be seen from Figure 4.17(b) that the calcination of titania(PVP) fibers without PAN core at 800 °C results in smooth fibers, which is different from the chain-like structure of the PAN/titania(PVP) co-axial fibers calcined at the same temperature. The difference in fiber structure indirectly confirms that PAN polymer was inside the fibers.



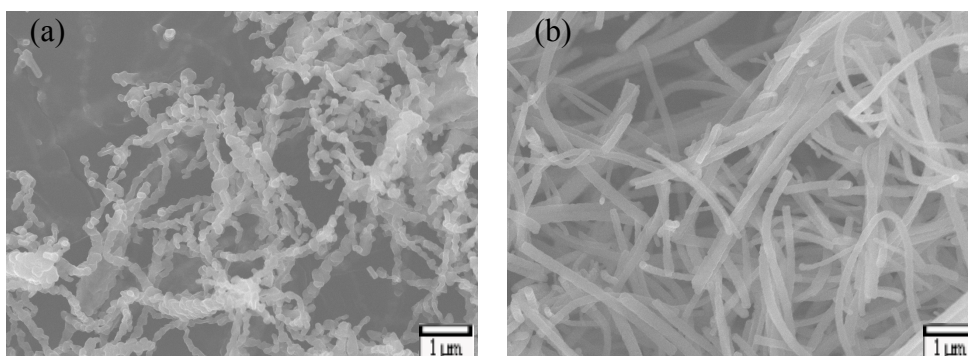


Figure 4.17 SEM images of 800 °C calcined fibers from PAN/TiO<sub>2</sub>(PVP) co-axial fibers (a) and from TiO<sub>2</sub>(PVP) simple fibers (b).

Figure 4.18 shows the average diameter of co-axial fibers after being calcined at different temperatures. The average fiber diameter does not change much at the calcination temperature of 300 °C, which is lower than the degradation temperature of both PVP and PAN. The decrease in the average diameter of the co-axial fibers is clearly observed when the calcination temperature is increased from 300 °C to 450 °C, which was found to be the range for PVP removal. After the calcination at 800 °C, the average diameter of fibers is decreased to be as low as 50 nm, which is expected to be the diameter of the residual titania fibers.

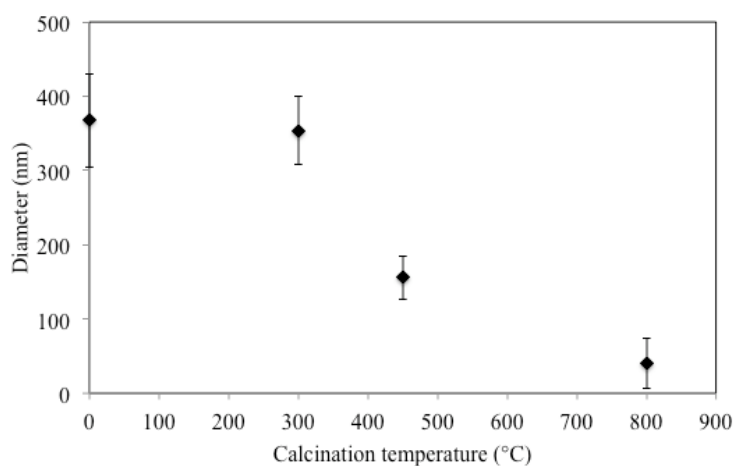


Figure 4.18 Diameter size with deviation of PAN/TiO<sub>2</sub>(PVP) co-axial fibers at different calcination temperature.

### 4.3.3 Observation of fiber cross section by TEM

Another way to confirm the core-sheath structure of the fibers is the observation of the fiber cross section. TEM images of the cross-section of PAN/titania (after calcination at 450 °C) co-axial fibers are investigated. It can be seen from Figure 4.19 that a core polymer is covered with titania particles. The particles are quite uniform with an average particle size of 4.3 nm and a standard deviation of 0.8 nm. For cross section sample preparation, it is necessary to cut the fibers by microtome. As the glass temperature transition ( $T_g$ ) of PAN is around 100 °C [49], which is higher than the temperature while cutting the fibers for cross-sectional observation. Therefore the non-circular shape observing from TEM image Figure 4.19(b) is considered not to be the deformation of polymer core while cutting. Nevertheless, it is expected to be the difference plane of cut fiber as shown in Figure 4.20, which results in the oval shape of cross sectional of fiber in TEM image.

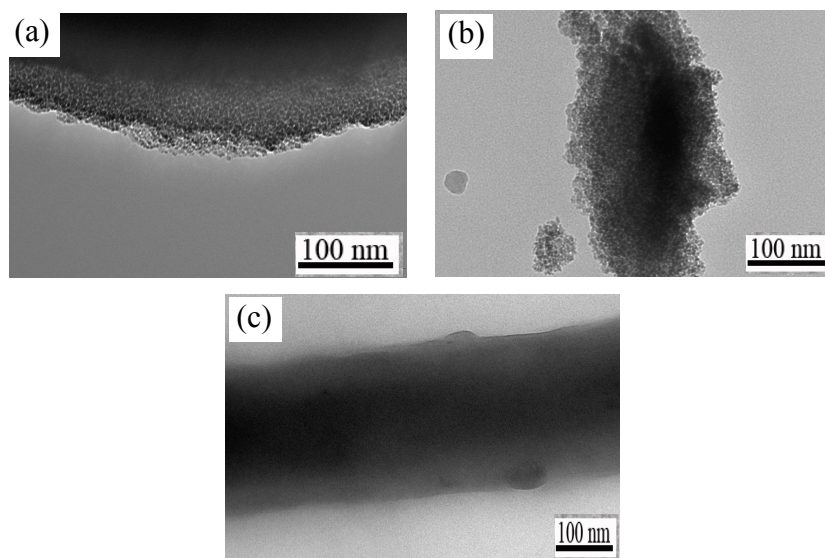


Figure 4.19 TEM image of cross-section of PAN/titania co-axial fiber (a-b), and PAN/titania coaxial fibers (c).

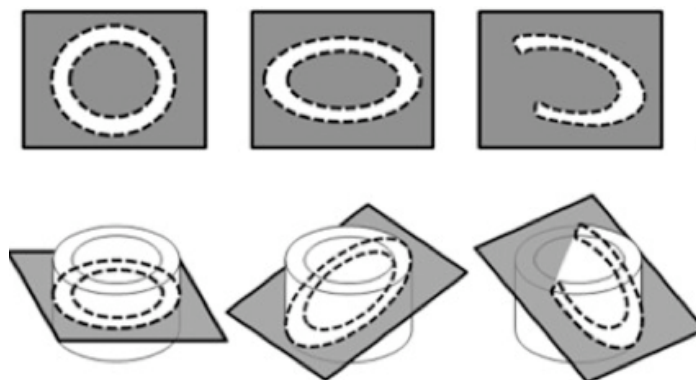


Figure 4.20 The possible cross sectional image of co-axial fibers

For this reason, core size observed from the cross section image, which is shown in Figure 4.19(b), is not exactly same as that shown in Figure 4.19(c) of co-axial PAN/titania. The fiber in the Figure 4.19(c) has a diameter of around 200 nm and in a cylindrical shape, which is difficult to see the titania grains in the sheath part clearly. Moreover, there is an objective lens below the sample and electrons of different energies are focused at different focal positions in TEM resulting in the well-known effect of chromatic aberration. This leads to blurring of the image and a loss of resolution and contrast. However, the difference between core and sheath parts still can be seen from this TEM image that the fibers. Beside, both core sizes observed from two ways are in a range of 80 to 100 nm.

Additionally, the cross section image of PAN/titania(PVP) was observed, Figure 4.21 shows the core-sheath structure of the fibers with no titania particle being found as Figure 4.19(a-b).

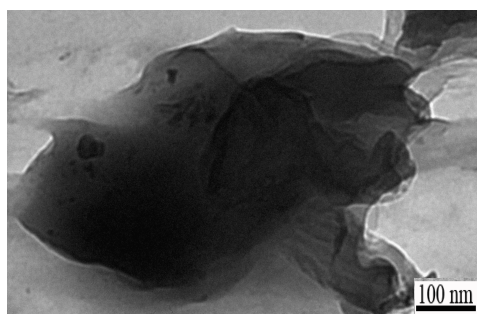


Figure 4.21 TEM image of cross-section of PAN/titania(PVP) as-spun co-axial fiber

#### 4.3.4 Fourier transform infrared spectroscopy (FT-IR) analysis

To confirm that core remaining in the fibers after calcination is PAN, the functional groups of electrospun products before and after calcination at 450 °C were investigated by FT-IR.

According to Figure 4.22(a), FT-IR spectra of PAN as-spun shows a signal corresponding to  $C\equiv N$  stretching at wavenumber around  $2244\text{ cm}^{-1}$ , besides, the bands at wavenumber around 2850, 2939, 1444, 1353, and  $1253\text{ cm}^{-1}$ , which are assigned to the aliphatic CH group vibrations of different modes in CH,  $CH_2$  and  $CH_3$ , respectively [48] are also observed. It can be seen from Figure 4.22(b-d) that when the calcination temperature is raised, the bands of aliphatic CH group vibrations are decreased due to the partial evaporation of small molecule from the polymers. Moreover, Figure 4.22(b-c) confirms the stabilization of PAN fibers when the fibers are heated up to 300 °C, which is previously explained in TGA/DSC thermogram. One of the most important reactions in the stabilization is cyclization, which is the reaction producing stable ladder polymer as shown in Figure 4.23. The cyclization can be confirmed by the fact that the intensity of  $C\equiv N$  stretching band is decreased when the calcination temperature is increased from 200 °C to 350 °C as shown in Figure (b-c), while new peak assigning to the stretching bond of  $C=N$  is presented at wavenumber of  $1590\text{ cm}^{-1}$ . Further heating up results in the conjugation in cyclic structure of PAN forming aromatic ring [50] as shown in Figure 4.23, which is confirmed by the band of aromatic  $C=C$  at wavenumber of  $810\text{ cm}^{-1}$  appearing in Figure 4.22 (c-d).

The band at  $1630\text{ cm}^{-1}$ , which appears only in the spectrum of as-spun fiber and 200 °C is assigned to be the stretching of  $C=O$  bond from the DMF solvent, which remains in fibers. The decrease of double peaks at 2340 and 2360 can be observed in the spectrum, which are assigned to be the decrease of the absorption of  $CO_2$  [51].

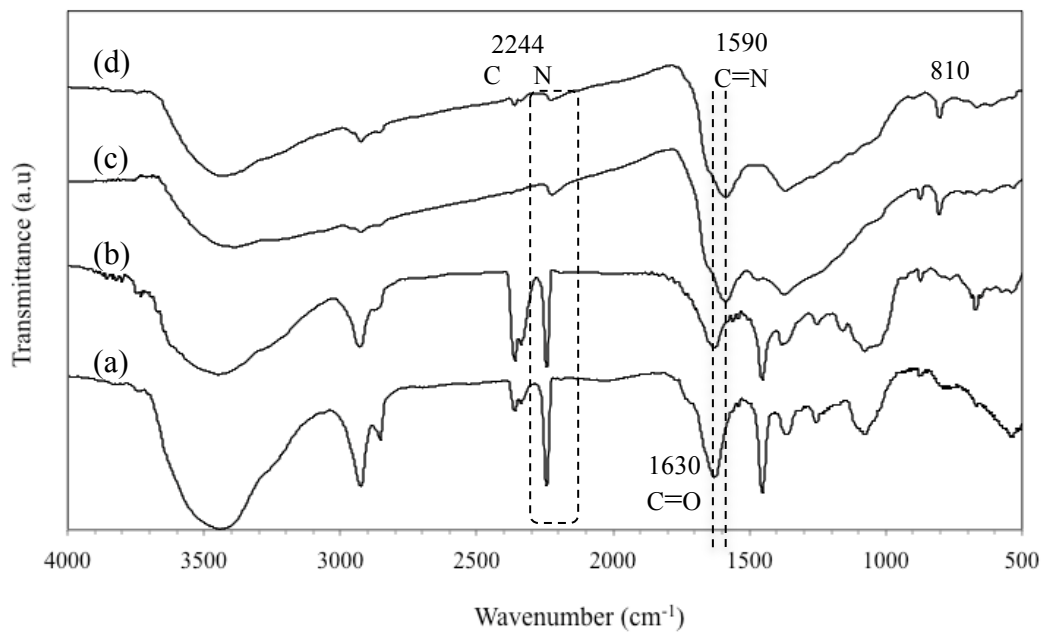


Figure 4.22 FT-IR spectrum of PAN as-spun fiber (a) and PAN pure fiber after calcination at 200°C (b), 350°C (c) and 400°C respectively.

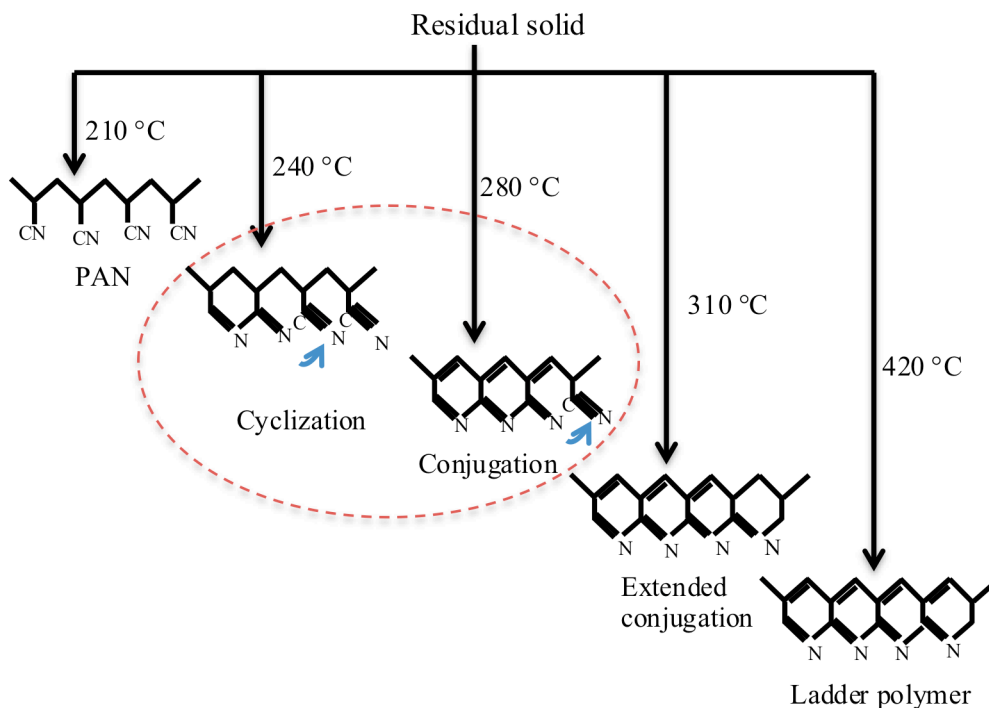


Figure 4.23 The possible degradative path and cyclization of PAN heated at various temperature proposed by Peikai Miao *et al* [50].

From Figure 4.24(c-d), FT-IR spectra of PAN/titania co-axial fibers is almost same as the spectra of PAN pure fiber after being calcined at 400 °C. It can be learned from this result that PAN in the core of fibers remains in the stable ladder polymer form after the calcination of the co-axial PAN/titania(PVP). However, the change of PAN does not affect the flexibility significantly, since the modified PAN is still a polymer. As the objective of this research is to synthesis the flexible fibers of titania, thus the change in molecular structure of PAN after calcination is acceptable. On the other hand, PVP in the sheath is removed after calcination as noticed in the absence of C=O bond at wavenumber of 1630  $\text{cm}^{-1}$ .

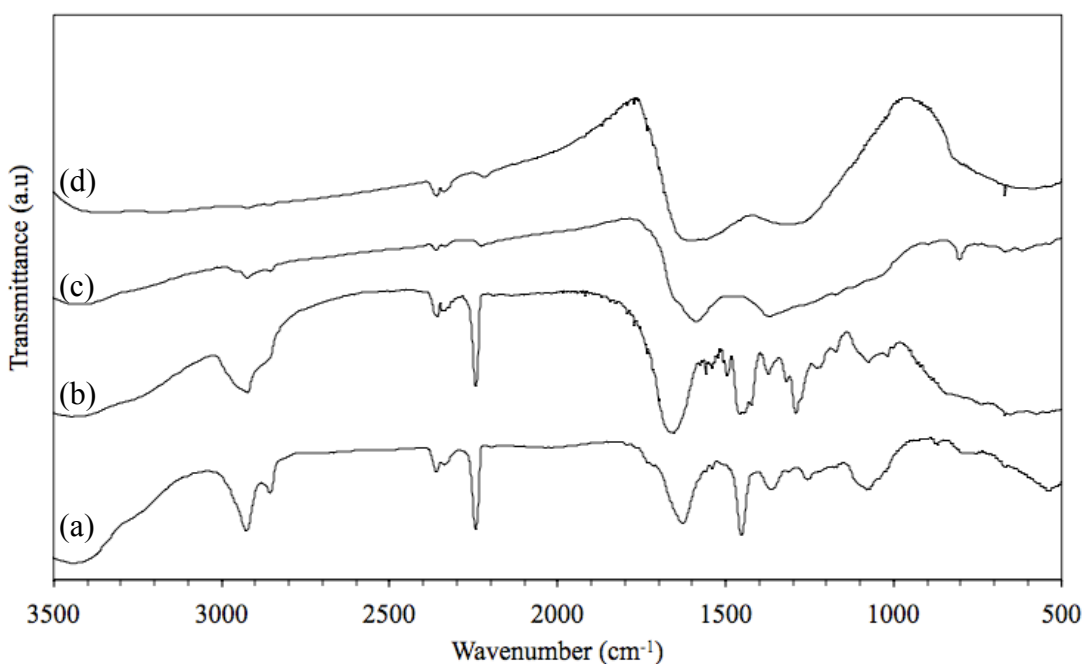


Figure 4.24 FT-IR spectrum of

- (a) : as-spun PAN pure fibers
- (b) : as-spun PAN/titania(PVP) co-axial fibers
- (c) : PAN pure fiber after calcination at 450 °C
- (d) : PAN/titania co-axial fibers after calcination at 450 °C

According to the low content of titania in the fibers, the FTIR spectra of PAN/titania co-axial fibers shows the band corresponding to PAN predominantly.

Beside, the FT-IR spectrum of the fiber after calcination shows the similar band to that of PAN fiber after calcination, thus only the change of polymers occurs without the interaction between core material and sheath material.

#### 4.3.5 Energy-dispersive X-ray spectroscopy (EDX)

To confirm that the particles observed in the sheath part of the fibers were titania, EDX analysis was used.

In agreement with TGA curve of PAN/titania(PVP) electrospun fibers, EDX results report that the product after calcination at 800 °C is titania with no polymer remained, which can be seen that no carbon element in fibers as shown in Figure 4.25.

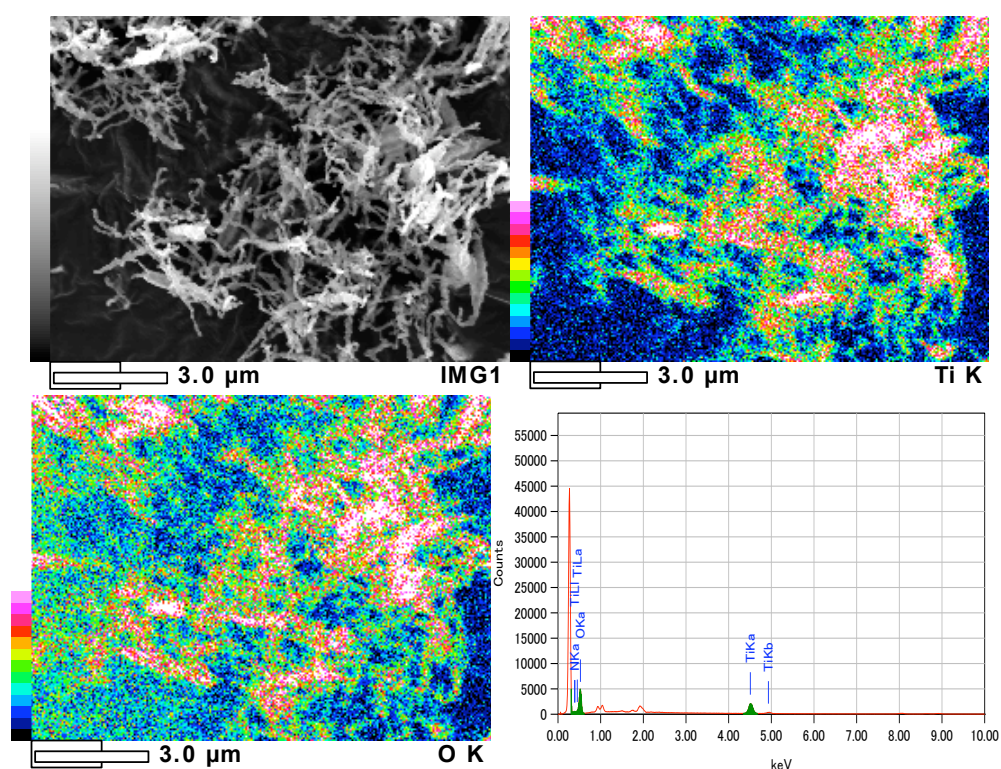


Figure 4.25 EDX map of  $\text{TiO}_2$  fibers after the calcination of PAN/ $\text{TiO}_2$ (PVP) at 800 °C.

The co-axial fibers after calcination at 450 °C were also analyzed by EDX. The result is shown in Figure 4.26. It can be seen that titania could also be obtained. Nevertheless, the presence of carbon also confirms the existence of the polymer core.



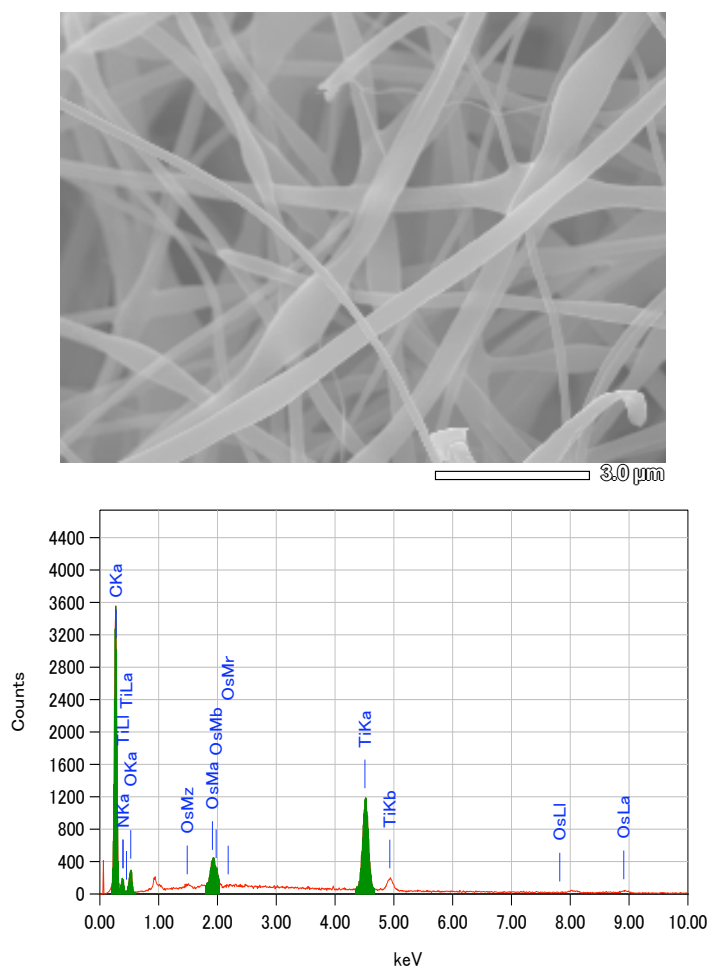


Figure 4.26 EDX analysis of PAN titania co-axial fibers after the calcination at 450 °C.

#### 4.4 Crystal Structure of Titania in Core-Sheath Fibers

After confirming that the PAN/titania co-axial fibers can be fabricated, the crystal structure of titania was investigated by X-ray diffraction (XRD). It can be confirmed that the calcination temperature of 450 °C is high enough to crystallize TiO<sub>2</sub> in the co-axial as-spun fibers to anatase as shown in Figure 4.27(a). The XRD patterns in Figure 4.27(a-b) show the presence of both anatase and rutile phases in the core-sheath products after the calcination. The fraction of anatase and rutile within the fibers depends on the temperature of calcination. Based on the equation described by Spurr and Myer (1957) [52],

$$F_r = 1 - \frac{1}{1 + 1.265 \frac{I_{\text{rutile}(110)}}{I_{\text{anatase}(101)}}}$$

where  $F_r$  is a fraction of rutile phase and  $I$  is an equivalent intensity of peak measured from XRD. The calculated content of rutile phase is increased from 0.34 to 0.4 with the increase in the calcination temperature from 450 °C to 500 °C respectively.

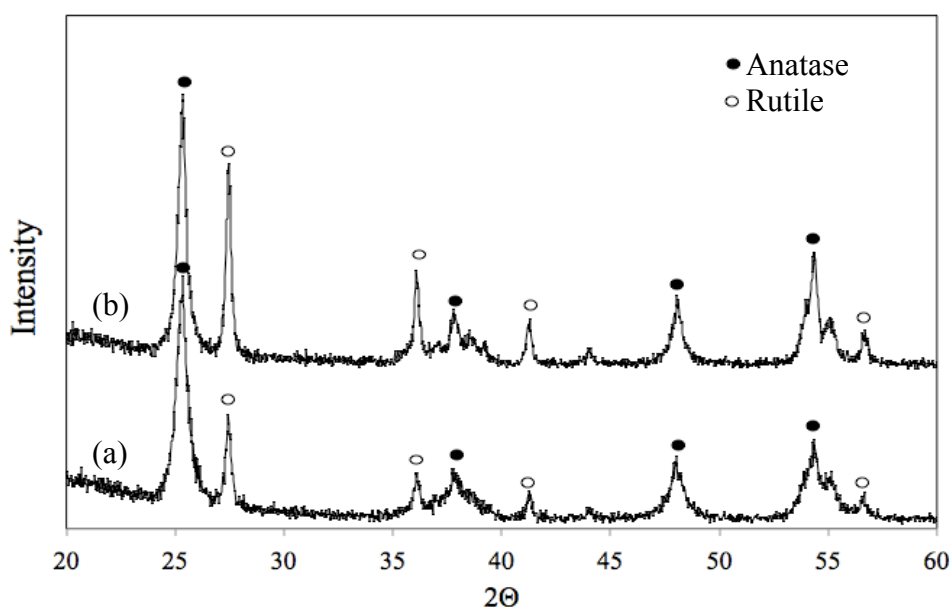


Figure 4.27 XRD patterns of the PAN/titania(PVP) core-sheath fibers calcined for 2 h at 450°C (a), and 500 °C (b) respectively.

Furthermore, it was found according to Figure 4.28 that the presence of DMF in the sheath solution also contributes to the formation of rutile phase. When ethanol was used as the solvent instead of DMF in the fabrication of PVP/titania nanofibers, only anatase phase is observed, as shown in Figure 4.28(a). Organic species, i.e., DMF in this case, induced the formation of smaller dimensions of the crystallites that leads to the decrease in the anatase-to-rutile phase transformation temperature [53]. It was proposed that organic solvent would produce the small crystallite of titania by reprecipitation effect leading to the decrease of phase transformation temperature. It was not clear about the reason why smaller crystallite size reduces the transformation temperature [54], only the experimental results shows that small crystallite size obtained. Therefore, further study about the mechanism of phase transformation in organic solvent added system is recommended.

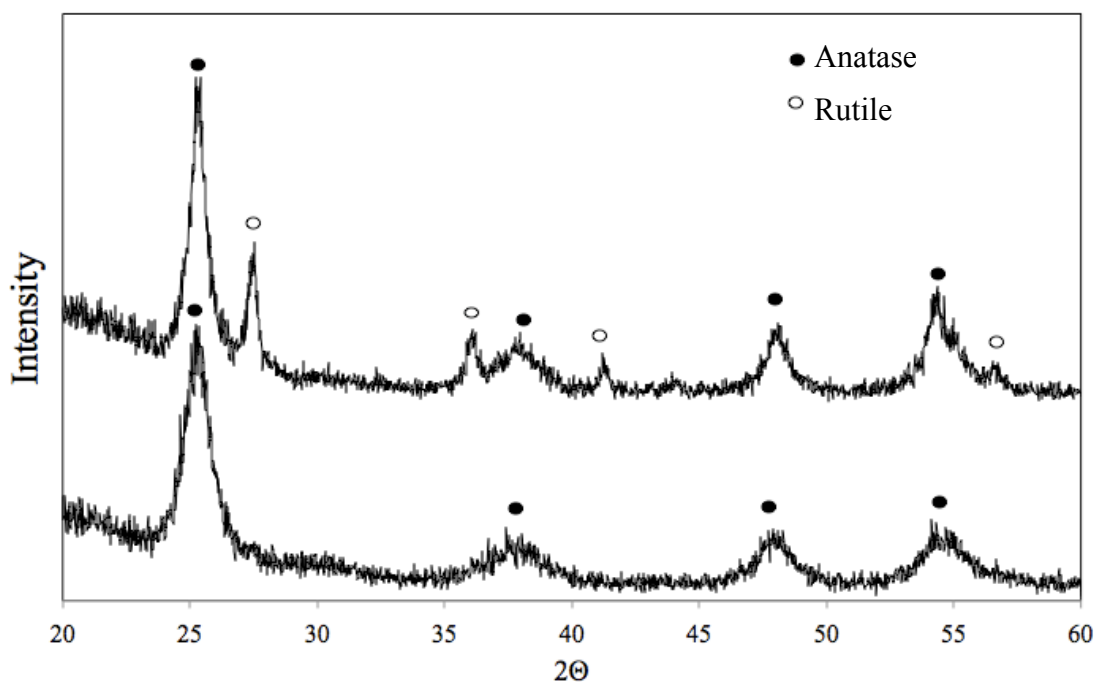


Figure 4.28 XRD patterns of the calcined PVP/titania fiber at 450 °C for 2h using EtOH (a), DMF (b) as a solvent in the spinning solution.

#### 4.5 Flexibility of PAN/TiO<sub>2</sub> Core-Sheath Fibers

Tensile strength of the fibers was analyzed to confirm flexibility of the co-axial fibers. Figure 4.29 shows stress-strain curves of PAN/titania(PVP) co-axial as-spun fibers and that of PAN/titania co-axial fibers obtained after calcination at 450°C for 2 h.

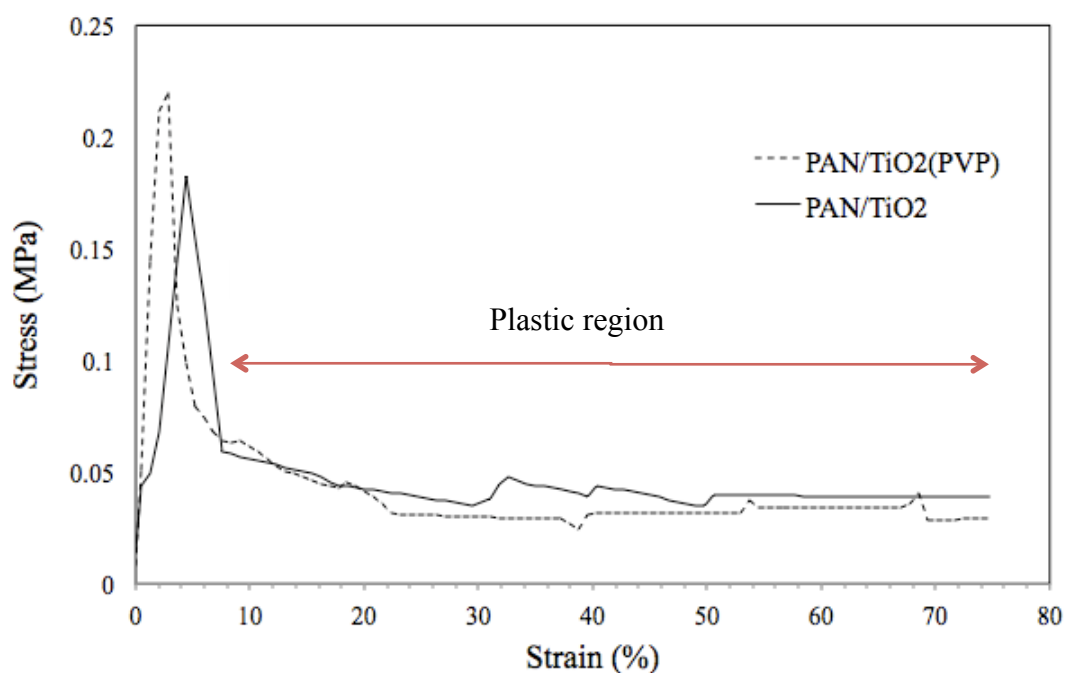


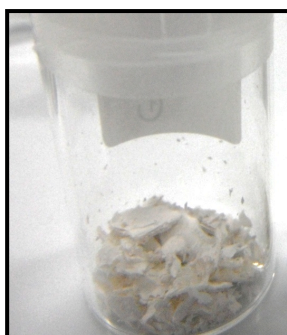
Figure 14.29 Stress-strain curves of PAN/TiO<sub>2</sub>(PVP) as-spun co-axial fibers and PAN/TiO<sub>2</sub> co-axial fibers.

Both fibers give the same pattern of curves having two regions, which represent the elastic region and plastic region. In elastic region, stress and strain are proportional. In this case, when a stress is applied and then removed, the fibers move back to their original position. For plastic region, permanent deformation occurs when stress is applied in this region. The curve starts from a linear elastic region reaching to the yield point, followed by a drop in stress, deformations of specimens of fibers, which is in the plastic region and finally fracture. This pattern represents a semi-crystalline polymer, which is consistent with property of PAN. Thus, it is confirmed that PAN core retains its mechanical properties, i.e., tensile strength, which refers the strength of the fibers. The measurement shows stress-strain curve of the sample. As

seen in the curve of both as-spun fibers and calcined fibers, the plastic region is still existed. This result informs that the fibers can be bent before its fracture, which is different from pure titania fibers that easy to be crumble in to powder as shown in Figure 4.30. In addition, the fibers can absorb tensile force even the fibers are not align in the same direction, thus the fibers can absorb force from any directions confirming its flexibility both before and after calcination.



(a)



(b)

Figure 14.30 PAN/titania co-axial fibers (a) and titania fiber (b) after calcinations at temperature of 450 °C.

It can be seen from Figure 14.30(a) that the sheet of fibers still can be obtained after calcination. According to the use of plate collector of an aluminum foil, the fibers were deposited on the plate, forming sheet of fibers. Hydrogen bond between the H atom and N or C atom in the sheath materials were formed, which fixed fibers together. Although polymer in the sheath part is removed after calcination, the nano size of fibers made the fibers being difficult to be separated naturally.

Considering the color of the products, it can be seen that the dark brown color of co-axial fibers are obtained after calcination. This can be explained by the transparency of titania nanograins covering the polymer core, which make the sheath of fiber been transparent. Thus, the color of the co-axial fiber is close to that of the core material.

Additionally, it is found that the yield strength of PAN/titania(PVP) fibers is higher than that of PAN/titania fibers according to the stabilization of PAN during calcination, which results in the decrease of yield strength of the fibers. On the contrary, there is no effect of PAN stabilization on the plastic region of the fibers as shown in the stress-strain curve.

## CHAPTER V

### CONCLUSIONS AND RECOMMENDATIONS

#### 5.1 Summary of the Results

1. PAN/TiO<sub>2</sub> can be fabricated from TiO<sub>2</sub> sol, which is prepared by sol-gel process, and PAN solution via co-axial electrospinning process followed by calcination.

2. Viscosity of the sheath solution has influences on surface of core/sheath structure of the co-axial electrospun fibers. In this work, high viscosity causes mixing between core and sheath solutions.

3. Flow rates of both core and sheath solutions affects the core-sheath structure of fibers, i.e., increasing sheath solution flow rate induces less defined core-sheath boundary of the fibers.

4. Voltage applied in the co-axial electrospinning has influence on the uniformity of the fiber products. High voltage results in no bead presence and high uniformity of the fiber products.

5. The diameter of the electrospun fibers depends on viscosity of solutions, flow rate of solutions, and voltage applied in the co-axial electrospinning process. The increase in fiber size is the result from an increase in of viscosity and flow rates of solutions. On the other hand, the increase of applied voltage results in the decrease in fiber size.

6. Flexible biphasic titania covered with PAN can be obtained after calcination at 450 °C.

#### 5.2 Conclusions

PAN/titania(PVP) co-axial nanofibers can be fabricated by the combination process of sol-gel and co-axial electrospinning technique. Viscosity of sheath solution, flow rates of both core and sheath solutions, and the applied electric potential are important processing parameters that affect morphology and size

distribution of as-spun fibers. Flexible biphasic titania fibers with PAN core can be obtained after calcination at 450 °C

### **5.3 Recommendations for the Future Studies**

Fabrication of PAN/titania co-axial nanofibers from PAN core solution and titania sol sheath solution by co-axial electrospinning process as well as effects of various factors, such as viscosity of spinning solutions, solution flow rates, electric potential applied, calcination temperature have been investigated in this research. There are some recommendations for future studies given below.

1. In order to make the aligned fibers, it is recommended to use rotating drum collector in the co-axial electrospinning process.
2. Effects of some environmental parameters such as humidity, temperature and airflow in hood case should be studied.
3. With the purpose of photodegradation application of titania, the photocatalytic activity of the flexible titania fiber product should be studied.



## REFERENCES

- [1] A. Fujishima and K. Honda. Electrochemical photolysis of water at a semiconductor electrode. *Nature*, 238, 7(1972) : 37-8.
- [2] T. Sato, Y. Yamamoto, Y. Fujishiro, and S. Uchida. Intercalation of iron oxide in layered  $\text{H}_2\text{Ti}_4\text{O}_9$  and  $\text{H}_4\text{Nb}_6\text{O}_{17}$ : visible-light induced photocatalytic properties. *Journal of the Chemical Society, Faraday Transactions*, 92, 1996.
- [3] S. Uchida, Y. Yamamoto, Y. Fujishiro, A. Watanabe, O. Ito, and T. Sato. Intercalation of titanium oxide in layered  $\text{H}_2\text{Ti}_4\text{O}_9$  and  $\text{H}_4\text{Nb}_6\text{O}_{17}$  and photocatalytic water cleavage with  $\text{H}_2\text{Ti}_4\text{O}_9/(\text{TiO}_2, \text{Pt})$  and  $\text{H}_4\text{Nb}_6\text{O}_{17}/(\text{TiO}_2, \text{Pt})$  nanocomposites. *Journal of the Chemical Society, Faraday Transactions*, 93, 1997.
- [4] N. Xu, Z. Shi, Y. Fan, J. Dong, J. Shi, and M. Z. C. Hu. Effects of Particle Size of  $\text{TiO}_2$  on Photocatalytic Degradation of Methylene Blue in Aqueous Suspensions. *Industrial & Engineering Chemistry Research*, 38, 2(1999) : 373-379.
- [5] E. T. Bender, P. Katta, G. G. Chase, and R. D. Ramsier. Spectroscopic investigation of the composition of electrospun titania nanofibers. *Surface and Interface Analysis*, 38, 2006 : 1252-1256.
- [6] C. Tekmen, A. Suslu, and U. Cocen. Titania nanofibers prepared by electrospinning. *Materials Letters*, 62, 2008 : 4470-4472.
- [7] W. Nuansing, S. Ninmuang, W. Jarernboon, S. Maensiri, and S. Seraphin. Structural characterization and morphology of electrospun  $\text{TiO}_2$  nanofibers. *Materials Science and Engineering: B*, 131, 2006 : 147-155.
- [8] C. Wang, Y. Tong, Z. Sun, Y. Xin, E. Yan, and Z. Huang. Preparation of one-dimensional  $\text{TiO}_2$  nanoparticles within polymer fiber matrices by electrospinning. *Materials Letters*, 61, 2007 : 5125-5128.

- [9] A. K. Moghe and B. S. Gupta. Co-axial Electrospinning for Nanofiber Structures: Preparation and Applications. *Polymer Reviews*, 48, 2008 : 25.
- [10] J. Wathanaarun, V. Pavarajarn, and P. Supaphol. Titanium (IV) oxide nanofibers by combined sol-gel and electrospinning techniques: preliminary report on effects of preparation conditions and secondary metal dopant. *Science and Technology of Advanced Materials*, 6, 5(2005) : 240-245, 2005.
- [11] S.-J. Lee, N.-I. Cho, and D. Y. Lee. Effect of collector grounding on directionality of electrospun titania fibers. *Journal of the European Ceramic Society*, 27, 2007 : 3651-3654.
- [12] A. K. Alves, F. A. Berutti, F. J. Clemens, T. Graule, and C. P. Bergmann,. Photocatalytic activity of titania fibers obtained by electrospinning. *Materials Research Bulletin*, 44, 2009 : 312-317.
- [13] L. Reijnders. Hazard reduction for the application of titania nanoparticles in environmental technology. *Journal of Hazardous Materials*, 152, 2008 : 440-445.
- [14] C. H. Kwon, H. Shin, J. H. Kim, W. S. Choi, and K. H. Yoon. Degradation of methylene blue via photocatalysis of titanium dioxide. *Materials Chemistry and Physics*, 86, 2004 : 78-82.
- [15] S. Farrokhpay, G. Morris, D. Fornasiero, and P. Self. Titania pigment particles dispersion in water-based paint films. *Journal of Coatings Technology and Research*, 3, 2006 : 275-283.
- [16] S. Inoue, H. Kodou, A. Muto, and T. Ono. Novel preparation of titania(TiO<sub>2</sub>) catalyst support by applying the multi-gelation method for ultra-deep HDS of diesel oil. *Fuel Chemistry Division Preprints*, 48, 2003 : 2.
- [17] Y. Xiao, J. Wu, G. Yue, G. Xie, J. Lin, and M. Huang. The preparation of titania nanotubes and its application in flexible dye-sensitized solar cells. *Electrochimica Acta*, 55 : 4573-4578.

- [18] P. Zeman and S. Takabayashi. Nano-scaled photocatalytic TiO<sub>2</sub> thin films prepared by magnetron sputtering. *Thin Solid Films*, 433, 2003 : 57-62.
- [19] "<Metal Oxide-Coated Polymer Fiber.pdf>."
- [20] Y. Hu, H. L. Tsai, and C. L. Huang. Phase transformation of precipitated TiO<sub>2</sub> nanoparticles. *Materials Science and Engineering: A*, 344, 2003 : 209-214.
- [21] Y.-H. Zhang and A. Reller. Phase transformation and grain growth of doped nanosized titania. *Materials Science and Engineering: C*, 19, 2002 : 323-326.
- [22] J.G. Santos, T. Ogasawara, and R. A. Correa. Synthesis of nanocrystalline rutile-phase titania at low temperatures. *Materials Science-Poland*, 27, 2009 : 10.
- [23] A. Fujishima, K. Hashimoto, and T. Watanabe. *TiO<sub>2</sub> photocatalysis : fundamentals and applications*. Tokyo: Bkc, 1999.
- [24] T. Wang and S. Kumar. Electrospinning of polyacrylonitrile nanofibers. *Journal of Applied Polymer Science*, 102, 2006 : 1023-1029.
- [25] M. Skotak and G. Larsen. Solution chemistry control to make well defined submicron continuous fibres by electrospinning: the (CH<sub>3</sub>CH<sub>2</sub>CH<sub>2</sub>O)<sub>4</sub>Ti/AcOH/poly(N-vinylpyrrolidone) system. *Journal of Materials Chemistry*, 16, 2006 : 3031.
- [26] M. Yoshida and P. N. Prasad, "Sol, Gel-Processed SiO<sub>2</sub>/TiO<sub>2</sub>/Poly(vinylpyrrolidone) Composite Materials for Optical Waveguides. *Chemistry of Materials*, 8, 1(1996) : 235-241.
- [27] G. Ertl, H. Knozinger, and J. Weitkamp, *Preparation of solid catalysts*: Wiley, 1999.
- [28] K. Y. Jung and S. B. Park. Anatase-phase titania: preparation by embedding silica and photocatalytic activity for the decomposition of trichloroethylene.

- Journal of Photochemistry and Photobiology A: Chemistry*, 127, 1999 : 117-122.
- [29] D. H. Reneker and A. L. Yarin. Electrospinning jets and polymer nanofibers. *Polymer*, 49, 2008 : 2387-2425.
- [30] Y.M. Shin, M.M. Hohman, M.P. Brenner, and G. C. Rutledge. Experimental characterization of electrospinning- the electrically forced jet and instabilities. *Polymer*, 42, 2001 : 13.
- [31] G. Srinivasan and D. H. Reneker. Structure and morphology of small diameter electrospun aramid fibers. *Polymer International*, 36, 1995 : 195-201.
- [32] D. Li and Y. Xia. Fabrication of titania nanofibers bby electrospinning. *Nano Letters*, 3, 2003 : 16.
- [33] A. Greiner, J. H. Wendorff, A. L. Yarin, and E. Zussman. Biohybrid nanosystems with polymer nanofibers and nanotubes. *Applied microbiology and biotechnology*, 71, 7(2006) : 387-93.
- [34] D. Li and Y. Xia. Direct Fabrication of Composite and Ceramic Hollow Nanofibers by Electrospinning. *Nano Letters*, 4, 5(2004) : 933-938.
- [35] A. K. Moghe and B. S. Gupta. Co-axial Electrospinning for Nanofiber Structures: Preparation and Applications. *Polymer Reviews*, 48, 2008 : 353-377.
- [36] F. Li;, Y. Zhao;, and Y. Song. *Core-Shell Nanofibers: Nano Channel and Capsule by Coaxial Electrospinning*. 2010.
- [37] I. G. Loscertales, A. Barrero, I. Guerrero, R. Cortijo, M. Marquez, and A. M. Ganan-Calvo. Micro/Nano Encapsulation via Electrified Coaxial Liquid Jets. *Science*, 295, 3(2002) : 1695-1698.

- [38] J. E. Diaz, A. Barrero, M. Marquez, and I. G. Loscertales. Controlled encapsulation of hydrophobic liquids in hydrophilic polymer nanofibers by co-electrospinning. *Adv. Funct. Mater.*, 16, 2006 : 7.
- [39] J. H. Yu, S. V. Fridrikh, and G. C. Rutledge. Production of Submicrometer Diameter Fibers by Two-Fluid Electrospinning. *Advanced Materials*, 16, 2004 : 1562-1566.
- [40] Y. Zhang, Z.-M. Huang, X. Xu, C. T. Lim, and S. Ramakrishna. Preparation of Core, Shell Structured PCL-r-Gelatin Bi-Component Nanofibers by Coaxial Electrospinning. *Chemistry of Materials*, 16, 9(2004) : 3406-3409.
- [41] C.-L. He, Z.-M. Huang, X.-J. Han, L. Liu, H. Ä. Zhang, and L. Ä. Chen. Coaxial Electrospun Poly(L-Lactic Acid) Ultrafine Fibers for Sustained Drug Delivery. *Journal of Macromolecular Science, Part B*, 45, 8(2006) 515-524.
- [42] Z. Sun, E. Zussman, A. L. Yarin, J. H. Wendorff, and A. Greiner. Compound Core-Shell Polymer Nanofibers by Co-Electrospinning. *Advanced Materials*, 15, 2003 : 1929-1932.
- [43] X. Yu, H. Xiang, Y. Long, N. Zhao, X. Zhang, and J. Xu. Preparation of porous polyacrylonitrile fibers by electrospinning a ternary system of PAN/DMF/H<sub>2</sub>O. *Materials Letters*, 64, 2010 : 2407-2409.
- [44] J. H. Song, J. H. Nam, J. H. Cho, B. I. Kim, and M. P. Chun. Microstructures and Multiferroic Properties of Electrospun BiFeO<sub>3</sub> Nanofibers. *Journal of the Korean Physical Society*, 20, 2012 : 6.
- [45] Haydn Kriel, Ronald D. Sanderson, and E. Smit. Coaxial Electrospinning of Miscible PLLA-Core and PDLLA-Shell Solutions and Indirect Visualisation of the Core-Sheath Fibres Obtained. *Fibres & Textiles in Eastern Europe*, 20, 2012 : 6.
- [46] N. Bhardwaj and S. C. Kundu. Electrospinning: a fascinating fiber fabrication technique. *Biotechnol Adv*, 28, 6(2010) : 325-47.

- [47] H. F. Moafi, A. Fallah Shojaie, and M. Ali Zanjanchi. Photoactivity Polyacrylonitrile Fibers Coated by Nano-Sized Titanium dioxide : Synthesis, Characterization, Thermal Investigation. *Journal of the Chilean Chemical Society*, 56, 2011 : 610-615.
- [48] A. V. Korobeinyk, R. L. D. Whitby, and S. V. Mikhalovsky. High temperature oxidative resistance of polyacrylonitrile-methylmethacrylate copolymer powder converting to a carbonized monolith. *European Polymer Journal*, 48, 2012 : 97-104.
- [50] P. Miao, D. Wu, K. Zeng, G. Xu, C. Ä. Zhao, and G. Yang. Influence of electron beam pre-irradiation on the thermal behaviors of polyacrylonitrile. *Polymer Degradation and Stability*, 95, 2010 : 1665-1671.
- [51] P. Yao Y Fau - Zhang, Z.-C. Zhang P Fau - Wang, Y.-H. Wang Zc Fau - Chen, and Y. H. Chen. Characterization of kale (*Brassica oleracea* var acephala) under thallium stress by in situ attenuated total reflection FTIR. 20090423 DCOM- 20100707.
- [52] R. A. Spurr and H. Myers. Quantitative Analysis of Anatase-Rutile Mixtures with an X-Ray Diffractometer. *Analytical Chemistry*, 29, 5(1957) : 760-762.
- [53] R. F. D. Farias, C. C. G. Silva, and T. A. G. Restivo. Thermal study of the anatase–rutile structural transitions in sol–gel synthesized titanium dioxide powders. *J. Serb. Chem. Soc.*, 70, 2005 : 5.
- [54] S. Yin, H. Hasegawa, and T. Sato. Phase-Compositional and Morphological Control of Titania Nanoparticles via Low Temperature Dissolution- Reprecipitation Process in Liquid Media. *Chemistry Letters*, 2002.

## **APPENDICES**

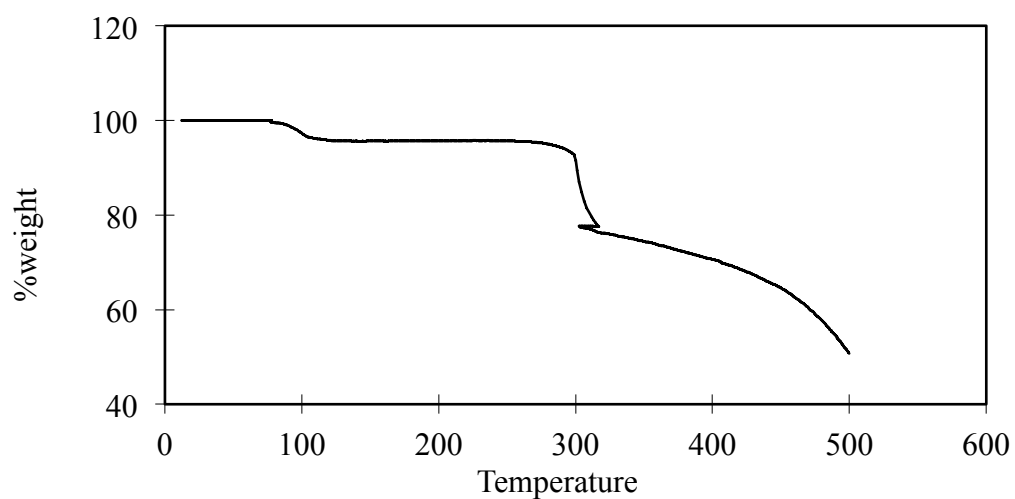
**APPENDIX A****TGA THERMOGRAMS OF PAN AND PVP**

Figure A.1 TGA thermogram of PAN fiber

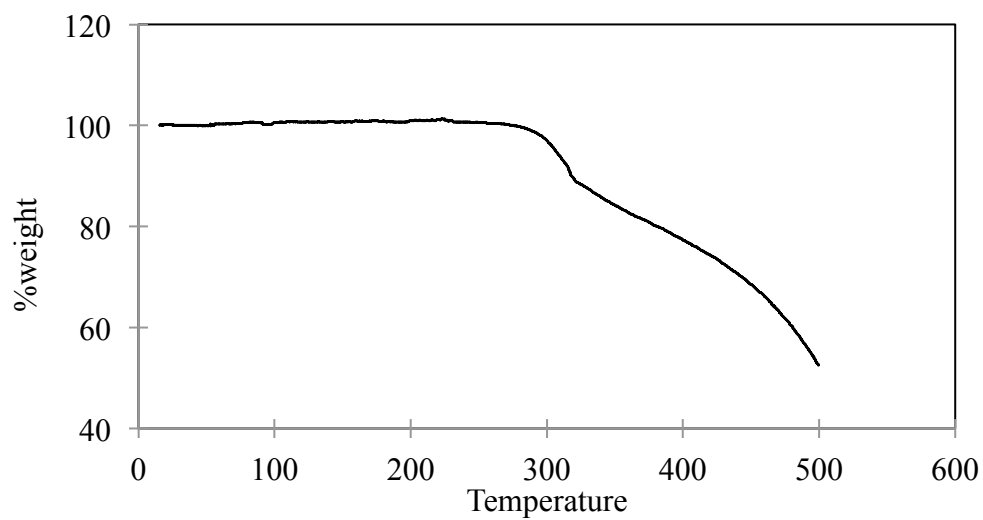


Figure A.2 TGA thermogram of PAN powder



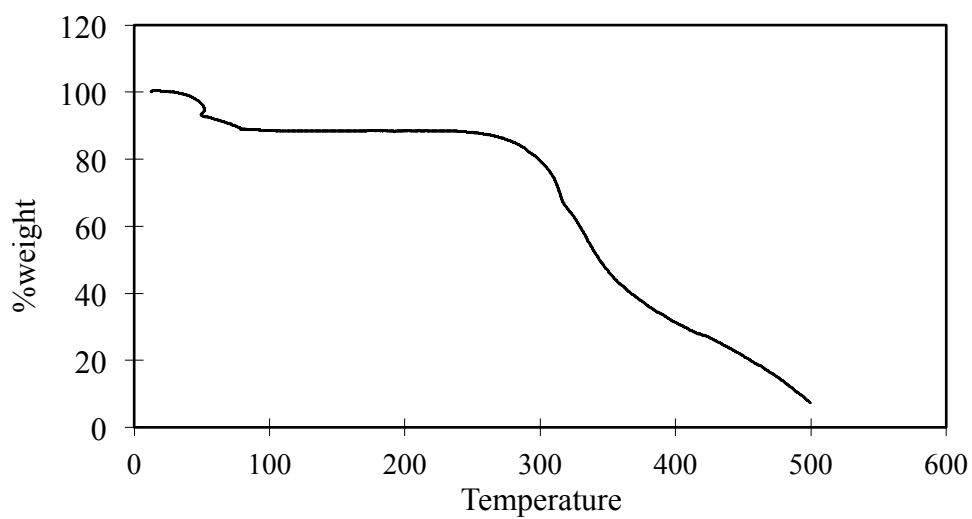


Figure A.3 TGA thermogram of PVP fiber

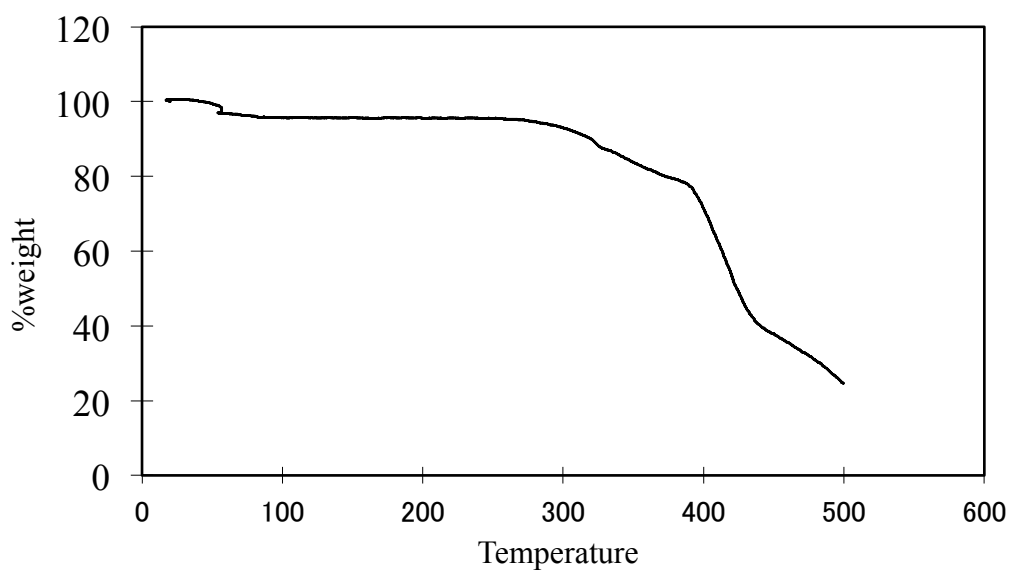


Figure A.4 TGA thermogram of PVP powder

**APPENDIX B**

**EFFECT OF TIME ON THE VISCOSITY OF SHEATH  
SOLUTION**

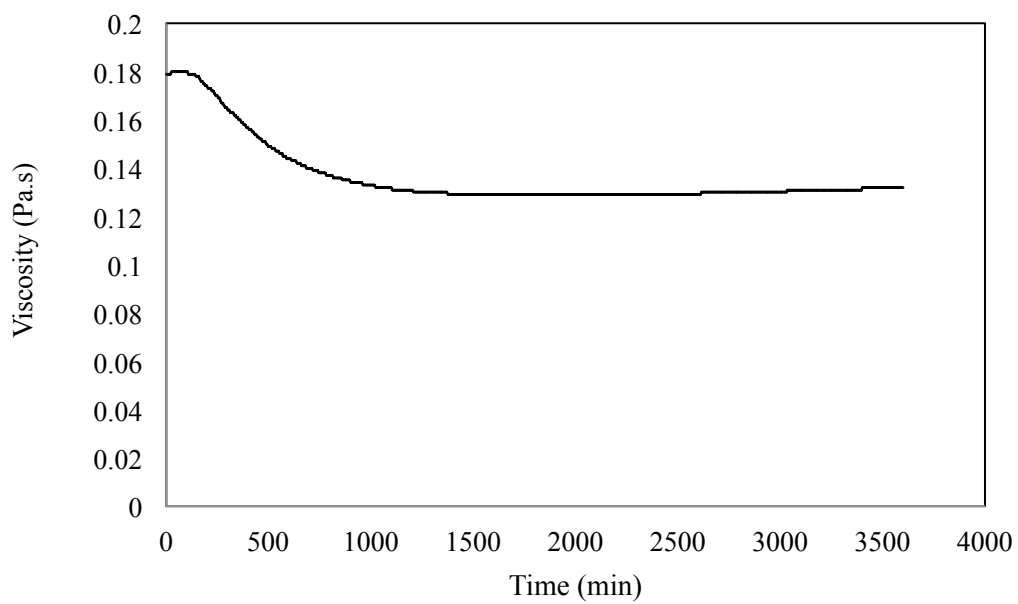
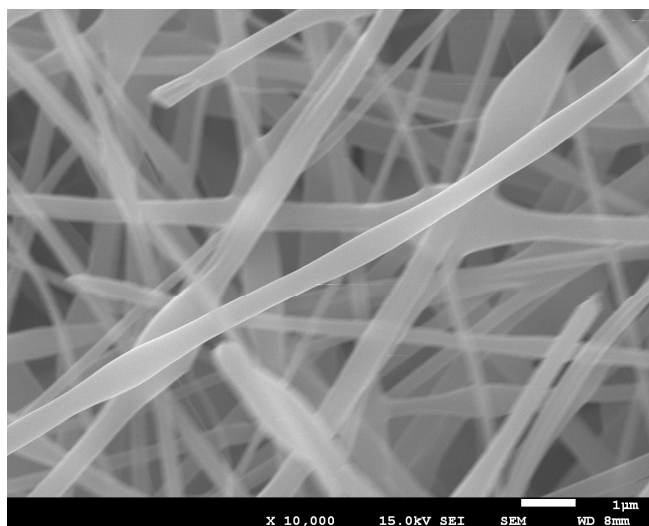


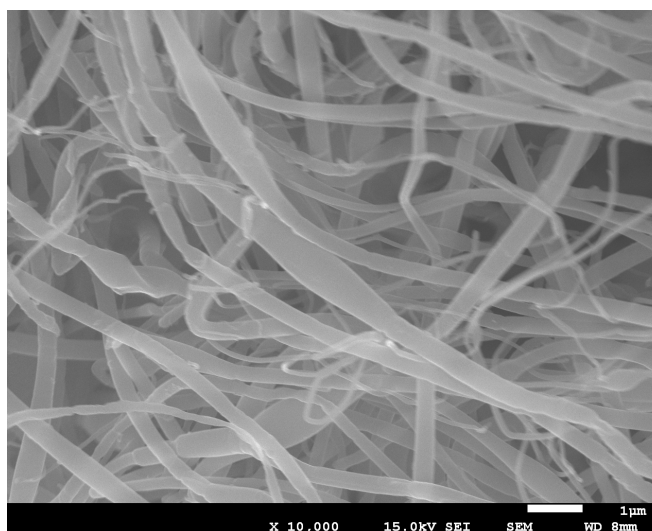
Figure B.1 Viscosity of titania(PVP) sheath solution

## APPENDIX C

### EFFECT OF AGING TIME OF SHEATH SOLUTION ON THE MORPHOLOGY OF FIBERS



(a)

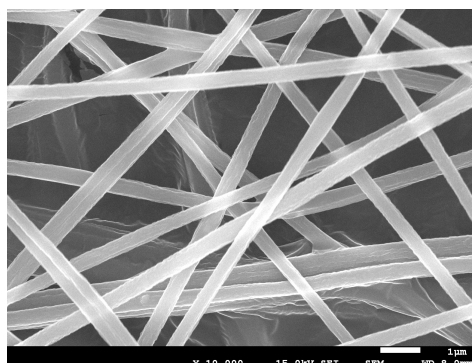


(b)

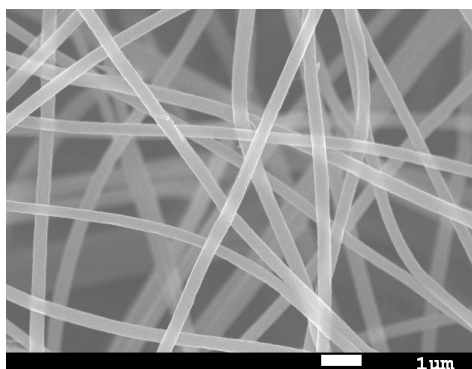
Figure C.1 SEM images of the products obtained from the co-axial electrospinning of PAN solution and PVP/titania solution using as prepared (a) and after aged for a day (b) before electrospinning process

## APPENDIX D

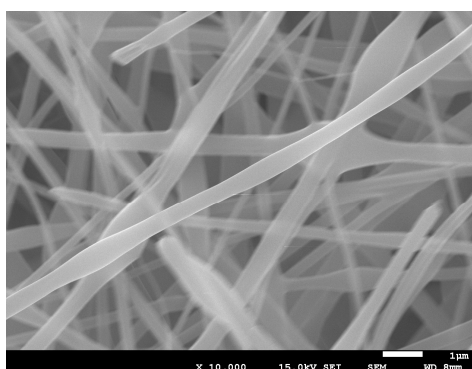
### EFFECT OF WORKING DISTANCE ON THE CO-AXIAL FIBER MORPHOLOGY



(a)



(b)



(c)

Figure D.1 SEM images of the products obtained from the co-axial electrospinning of PAN solution and PVP/titania solution with the applied electric voltage of 22 kV and the tip-to-collector distance are 16 cm (a), 19 cm (b), 22 cm (c) respectively

**APPENDIX E**

**EFFECT OF ROTATING DRUM COLLECTOR ON FIBERS  
MORPHOLOGY**

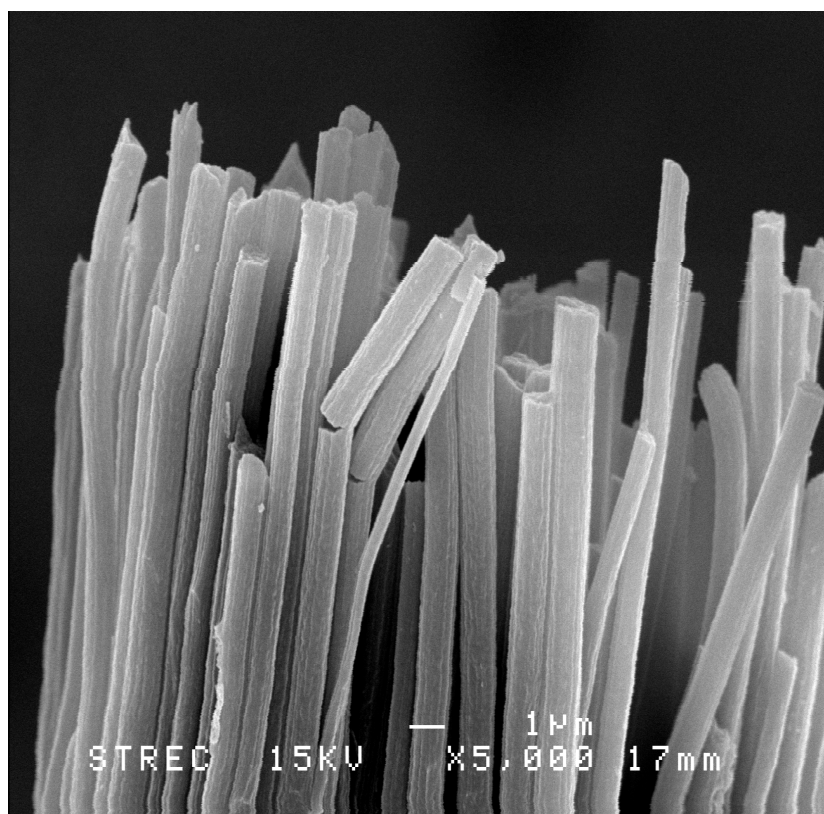


Figure E.1 PAN/titania co-axial fibers using rotating drum collector

## **APPENDIX F**

### **LIST OF PUBLICATION**

1. Farkfun Duriyasart, Masayoshi Fuji, Takashi Shirai, Chika Takai and Varong Pavarajarn, “fabrication of titania/polyacrylonitrile core-sheath nanofibers by electrospinning technique”, The 4th KKU International Engineering Conference 2012 (KKU-IENC 2012), Khon Kaen University, Thailand, May 10-12, 2012

## VITA

Miss. Farkfun Duriyasart was born on 5<sup>th</sup> December, 1987, in Nakornratchasima, Thailand. She received the Bachelor's Degree of Engineering with a major in Chemical Engineering from Chulalongkorn University, *Bangkok* in April 2010. She continued her Master study in the major in Chemical Engineering at Chulalongkorn University, Bangkok, Thailand in May 2010.